



**UNIVERSITY OF DEBRECEN
FACULTY OF ENGINEERING
DEPARTMENT OF
MECHANICAL ENGINEERING**

**GEOMETRIC DESIGN OF A BICYCLE
CHAIN TRANSMISSION
THESIS**

Li Yifei
Production Engineering Specialization

Debrecen
2026

Table of Contents

Table of Contents	I
Table of notations	III
Table of Glossary	V
Introduction	1
1 Literature Review	2
1.1 Bicycle basic theory	2
1.1.1 Bicycle history	2
1.1.2 Bicycle classification	3
1.1.3 Current status of bicycle biomechanics research	6
1.1.4 Research Status of Bicycle Shape Design	7
1.2 Bicycle composition	9
1.2.1 Main parts of a bicycle	9
1.2.2 Bicycle chain transmission	10
1.2.3 Crank and sprocket	12
1.2.4 Chain Drive Assembly	12
1.2.5 Research Status of New Bicycle Transmission Mechanisms	13
2 Design the chain transmission connection	16
2.1 Basic Introduction to Roller Chains	16
2.2 Chain selection	17
2.3 Roller chain modeling and assembly	19
3 Design CAM for the front sprocket	22
3.1 Model Preprocessing and CAM Environment Construction	22
3.1.1 Model Preprocessing	22
3.1.2 CAM environment setup	22
3.2 Machine tool model selection	23
3.3 Simulation settings	27
4 Design CAM for the back sprocket	34
4.1 CAM Environment Construction	34
4.1.1 CAM environment setup	34

4.2 Machine tool model selection	36
4.3 Simulation settings	36
5 FEM Analysis for the chain transmission	48
5.1 Finite Element Theory Foundation	48
5.2 Geometric modeling and material property setting	48
5.2.1 Ansys Analysis	49
5.2.2 Material Assignment	50
5.2.3 Model Import	51
5.3 Grid Division and Boundary Conditions	52
5.3.1 Grid division	52
5.3.2 Boundary condition setting	52
5.4 FEM analysis	55
5.4.1 Static analysis	55
5.4.2 Modal analysis	55
6 Conclusion	59
List of references	62

Table of notations

v_c	$\left[\frac{m}{s}\right]$	Chain speed
v_{bike}	$\left[\frac{m}{s}\right]$	Bike speed
d_{wheel}	[mm]	The tire diameter
n_1	$\left[\frac{r}{min}\right]$	Pedaling speed
$m_{bike\ mass}$	[kg]	The bicycle weighs
π		Pi (3.14)
n_2	$\left[\frac{r}{min}\right]$	Rear wheel speed
i		Transmission ratio
z_1		Number of teeth of large gear
z_2		Number of teeth of smaller gear
$m_{human\ mass}$	[kg]	The human weighs
F_N	[N]	Total pressure of people and vehicles on the ground
f		The coefficient of friction
F_f	[N]	Total friction between the ground and people and bicycle
P	[kW]	Power transferred
P_{ca}	[kW]	Calculate power
p	[mm]	Pitch
K_A		Operating condition coefficient
K_Z		Small sprocket gear coefficient
a_0	[mm]	Center distance
L_p		Chain length number of links
F_e	[N]	Effective circumferential force
a	[mm]	Maximum center distance
K_{FP}		The coefficient of the axial force when the sprocket is horizontal
F_p	[N]	Axial force
T	[N·m]	Torque of rotation
m		Mass matrix

c	Damping matrix of the system
k	Stiffness matrix of the system
x	The displacement of the system
f	The motivating force of the system.

Table of Glossary

CAE	Computer-Aided Engineering
CAD	Computer-Aided Design
CAM	Computer Aided Manufacturing
FEM	Finite Element Method

Introduction

In recent years, environmental pollution has become increasingly serious, once again prompting people to deeply reflect on the choice and use of transportation methods. At the same time, with the upgrading of residents' consumption structure and the improvement of consumption level, people pay more attention to the structure, function, safety and quality of bicycle products. Therefore, the bicycle industry should constantly innovate to meet people's usage needs. From the bicycles of the early 19th century to today's complex ones, this simple yet elegant machine has undergone astonishing evolution, adapting to the constantly changing demands of society and technological progress. In recent decades, with the growing global concern over environmental sustainability, traffic congestion and public health issues, bicycles have regained popularity. They are no longer merely means of transportation, but have developed into symbols of green living, fitness tools, and even competitive sports. According to the latest statistics, the global population of cyclists continues to grow at an unprecedented rate, and bicycles have gradually become a key solution for many cities to alleviate traffic congestion and reduce carbon emissions. The enduring popularity of bicycles can be attributed to their unique combination of simplicity, efficiency and multi-functionality. Unlike motor vehicles, bicycles do not require fossil fuels, produce no emissions and have the least impact on the environment. They offer an affordable and convenient means of transportation for people of all ages and backgrounds, while also providing significant health benefits through physical exercise. However, although it seems simple on the surface, a bicycle is a complex mechanical system that relies on the precise interaction among its various components to function effectively. Among these components, the chain drive system stands out as the heart of the bicycle, responsible for converting the rider's pedal force into forward motion. This system is composed of chains, sprockets, cranks and related components, and plays a crucial role in determining the performance, efficiency and overall riding experience of the bicycle.

1 Literature Review

This article will review the historical development and evolution of bicycles, analyze their core structural components and working principles, and introduce the various mechanisms and basic components of bicycle transmission systems. The article will also focus on the selection and design innovation of transmission systems.

This article mainly designs the chain drive system of bicycles. After modeling with 3D software, finite element analysis is conducted to verify the rationality of the design.

1.1 Bicycle basic theory

1.1.1 Bicycle history

If we ask ourselves when the bicycle originated, perhaps we should go back to Ancient Egypt. Throughout history, hieroglyphs like those on the Luxor Obelisk in Paris have been found, illustrating names mounted on a horizontal bar supported by two wheels for movement. Similar figures have also been found in Roman frescoes in the volcanic city of Pompeii, and even sketches by Leonardo da Vinci that closely resemble the bicycle of today.

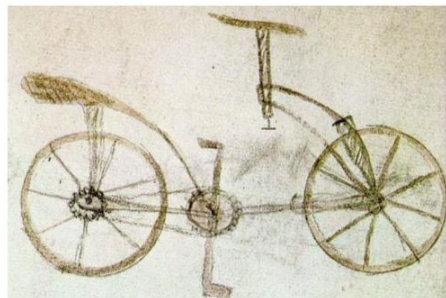


Figure 1.1. Da Vinci's Manuscripts[1]

At the beginning of the 19th century, the Scotsman Kirkpatrick MacMillan created the first bicycle realistically maneuverable by one person using pedals, rather than propelling themselves with their feet on the ground as had been done until then. From this first model, successive innovations and improvements were made to the motion transmission system, and in 1864 the bicycle with a transmission capena was invented.

After many innovations and variations of MacMillan's original model, in 1885 the Briton John Starley Kemp, considered the father of the modern bicycle, created the 'Rover Safety Bicycle', with two wheels of the same radius, chain and

gear transmission, pedals and a sloping fork, models from which modern bicycles have been developed.

Eleven years later, and after the successful invention of the pneumatic tire, cycling was declared an Olympic sport in the first Olympic Games of the modern era.



Figure 1.2. ROVER SAFETY BICYCLE[2]

Since then, the bicycle has evolved into what we know today: a true engineering masterpiece, backed by thousands of studies, and has become one of the most widely used modes of transportation in the world.

There are multiple high-level cycling disciplines, the two most well-known and standardized being mountain biking and road cycling. Several Spaniards have excelled in both disciplines throughout history, including José Hermida, a multiple-time world mountain biking champion.



Figure 1.3 JOSÉ HERMIDA'S BICYCLE IN 2014[3]

1.1.2 Bicycle classification

The bicycle is a common land means of transportation, mainly driven by a person's legs. It is also known as a stationary bike or a bicycle and is an

indispensable means of transportation for people. Through extensive data collection and statistics, bicycles can be classified into the following major categories based on their different usage scenarios: mountain bikes, race bikes, recreational bikes, electric bikes, and other types of bicycles

The first category is mountain bikes, a type of bicycle used for traveling on rough mountain roads. Riders using this type of bicycle can travel steadily on roads with harsh environments.

(1) Mountain biking: Mainly used for mountain biking sports and mountain biking events, it is mainly targeted at mountain road areas. Therefore, the riding distance of this type of bicycle is required to be longer and the speed is required to be faster. At the same time, to meet the requirements of a more comfortable riding posture, the position of its handlebars is generally lower.

(2) Shock-absorbing mountain bikes: Generally used on roads with extremely poor environments, they are required to have good downhill performance, but their climbing performance is relatively poor. As they are used in mountainous areas, high shock absorption requirements are placed on the bikes. This type of bicycle is heavier than an ordinary mountain bike, also due to the shock absorption system it is equipped with.

(3) Extreme mountain bikes: Mainly used for extreme mountain bike sports, this type of bike has very strict requirements for its shock absorption performance. Therefore, not only is it necessary to be equipped with front and rear shock absorption systems, but also the shock absorption stroke needs to be increased. At the same time, the foot pedal is self-locking to ensure that it will not separate from the foot pedal when the vibration is large.

(4) Climbing bicycles: They are generally used in climbing competitions. The difference lies in that it is equipped with multiple levels of gears, does not have shock absorption function, and the vehicle body weight is relatively light. However, it has relatively high requirements for dynamic performance.

(5) Single-speed vehicles: Mainly suitable for relatively flat roads. Its main feature is a more fashionable design, but it generally does not have shock absorption or gear shifting functions. Its frame is made of all steel. In the design of the frame, emphasis is placed on the lightweight design of the frame.

The second category is competition bicycles, whose main features are light and easy riding, light weight and high body strength. The frame of its bicycle is mainly designed in a rhombic structure, and there are different heights to choose from, mainly based on the athlete's body type, and can also be customized according to the athlete's special needs.

(1) Road bike: This type of bike is mainly used for long-distance races on the road. Its large wheel diameter and narrow tires enable the bike to withstand extremely low riding resistance, resulting in a very high riding speed. Generally, they are equipped with external gear shifting mechanisms, bicycle brakes, chain

shifting devices, etc. However, this type of bicycle is not exactly the same as ordinary bicycles. It does not have components such as mudguards and brackets.

(2) Track cycling: As the name suggests, it is mainly used in track cycling competitions. Its shape is very similar to that of a road bike, but there are also differences. Its bicycle structure is simpler and it does not have the brakes and related gear shifting mechanisms of a road bike. When riding, track bikes cannot move backward or stop at will like ordinary bikes.

The third category is leisure bicycles, which are mainly developed for urban leisure, tourism and fitness purposes. These bicycles mainly serve the function of transportation and meet users' basic leisure needs.

(1) Urban leisure bicycles: Mainly serving as a means of transportation for urban residents, they have a relatively simple structure and are easy to maintain. They can meet the basic cycling needs of urban residents and also solve the problem of the "last mile" in urban transportation.

(2) Urban public bicycles: The public bicycle system mainly serves the city. Urban public bicycles are set up in areas with relatively concentrated foot traffic. Each area is equipped with bicycle rental stations, and a certain number of bicycles are placed at each rental point. Bicycles can be dispatched according to the situation of urban public transportation. Its structure is simple and maintenance is convenient.

(3) Travel bicycles: The humanized frame design is a feature of travel bicycles. These bicycles mainly use steel frames, which are suitable for long-distance riding and can also be used for daily commuting. This bicycle features high strength, large carrying capacity and strong durability. Meanwhile, travel bicycles are also designed in tourist attractions and parks to provide people with transportation services.

(4) Exercise bicycle: A type of bicycle that mainly relies on cycling for fitness. Exercise bikes usually involve coordinated movements of hands and feet. They can achieve single arm or leg movements, as well as simultaneous arm and thigh movements. This not only increases the riding speed but also exercises the muscles of the rider's legs and arms. It can be used as a mobility vehicle for the elderly as well as for fitness and entertainment.

The fourth category is electric bicycles, which mainly use batteries as energy sources. They are equipped with control components such as electric motors and controllers, and are also provided with display instruments. According to the riding mode, they can be divided into two types: automatic type and power-assisted type.

(1) Electric automatic bicycle: It mainly relies on electricity for driving and does not provide a way to drive by human power. It belongs to fully electrically driven bicycles.

(2) Electric-assisted bicycles: Compared with self-propelled bicycles, the most significant difference lies in that they can be driven by both human power and

electricity. They can be driven either by human power or by electric power depending on the situation.

The fifth category is other bicycles, mainly including foldable bicycles, children's bicycles, emerging shared bicycles and other types of bicycles.

(1) Folding bicycles: This type of bicycle also comes in various forms based on different user needs. It mainly optimizes the space occupied by the bicycle by folding the frame, and has the advantages of small space occupation and easy carrying.

(2) Children's bicycles: This type of bicycle is mainly used for children's entertainment. It mainly comes in two types: double-wheel or with auxiliary wheels.

(3) Shared bicycles Shared bicycles, also known as shared bikes, mainly include brands such as Mobike, Qiguo Bike, Meituan Bike, and Hellobike. This type of bicycle is a perfect combination of Internet technology and bicycles. When people need to use them, they can simply scan the code with their smartphones to ride. They are priced by the hour. The biggest difference from ordinary bicycles lies in the design of the lock. It also has the advantages of easy parking and convenient use.

1.1.3 Current status of bicycle biomechanics research

In international research, Soden et al.[4]. were the first to analyze pedal force in bicycles, ultimately concluding that the maximum value reached three times the rider's weight. Ray et al.[5] examined angular acceleration of the rider's thigh and lower leg, the force output from these segments, and the torque at various joints. Getz et al.[6] developed an extremely simplified bicycle dynamics model based on geometric mechanics, using it as a foundation to study bicycle control problems.

Boyer and Porez et al.[7] investigated bicycle dynamics from a geometric mechanics perspective and established a dynamic model of the bicycle using a general reduction method. Basu-Mandal et al.[8] employed Newton-Euler equations and the Euler-Lagrangian approach, combined with computer symbolic computation, to derive a complete nonlinear system of differential-algebraic equations for the Whipple bicycle. They verified the equivalence of the two models through numerical analysis.

In domestic research, Zhang Jian et al.[9] studied cyclists to analyze their pedaling motions during cycling, providing further scientific basis for coaches to guide athlete training. Wu Shangsheng et al.[10] proposed a human-bike integrated linkage model based on the physiological characteristics of the human lower limbs. Using data and model parameters, they established the kinematic and dynamic equations for this linkage model, completing the preliminary design of a new bicycle. Based on dynamic theory, Cong, Chen et al.[11]described bicycle

motion as two submodels: stability and vibration. Building on this, they analyzed bicycle movement under complex road conditions and developed a simulator to obtain key data.

1.1.4 Research Status of Bicycle Shape Design

As living standards improve, more and more people are beginning to pursue their emotional needs and the humanization of products to enhance the user experience. Consequently, research on bicycle design aesthetics is also advancing both domestically and internationally.

American designer Erik Stoddard created an electrically powered hybrid recumbent bicycle, which received an Excellence Award at the 2010 International Bicycle Design Competition, as shown in Figure 1.4. In terms of design, this bicycle incorporates ergonomics, mimicking the seating position of a small SUV. Therefore, the bicycle is more upright than traditional models, resulting in a more comfortable riding experience. Furthermore, the front wheel is pedal-driven, while the rear wheel is driven by a motor. The shortened wheelbase significantly increases maneuverability.



Figure 1.4 AutoVelo Hybrid Horizontal Bicycle[12]

In 2004, Blair Hasty in Europe designed and manufactured a prone bicycle using biomimetic principles, as shown in Figure 1.5. The pedals were moved from below the rider to the rear wheel, allowing the rider to lie prone on the bicycle. This streamlined design can reduce unnecessary tension in the lower back, hands and hips. In addition, for ease of use, this bicycle is designed with a foldable structure to meet the needs of most commuters.



Figure 1.5 Recumbent Bicycle[13]

According to domestic research, Li Wenhao et al[14] analyzed the emotional needs of astronauts from a psychological perspective by examining the harshness of the space environment. They proposed a design model based on emotional needs and, integrating the proposed methodology, completed the design of a bicycle for space fitness, as shown in Figure 1.6. Xia Lichao[15] and colleagues focused on children's bicycles, analyzed the market, identified multiple essential design elements, and developed a design that simultaneously meets the requirements for children's bicycles, tricycle balance bikes, and children's walkers, as shown in Figure 1.7. This design also accommodates the usage needs of children across different age groups.

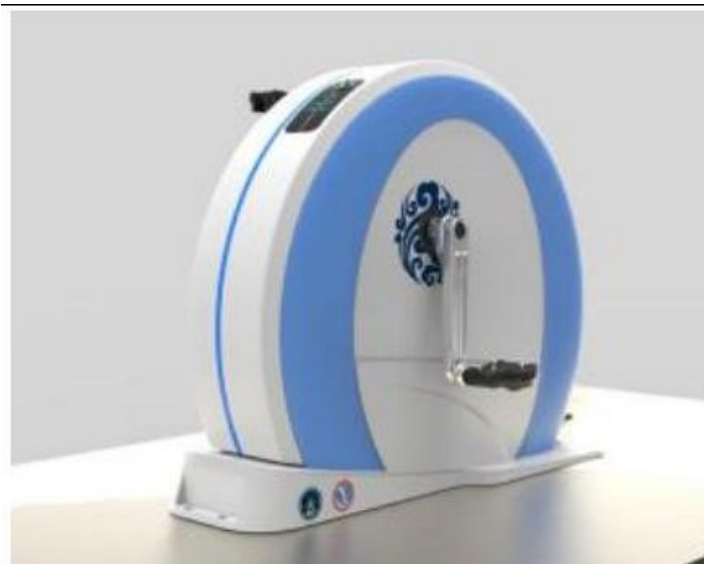


Figure 1.6 Space Fitness Bicycle[14]



Figure 1.7 Multifunctional Children's Bicycle[15]

1.2 Bicycle composition

1.2.1 Main parts of a bicycle

The primary function of a bicycle is to propel itself forward using the rider's legs. To accomplish this, each component of the bicycle must function independently and work together to achieve the riding function.

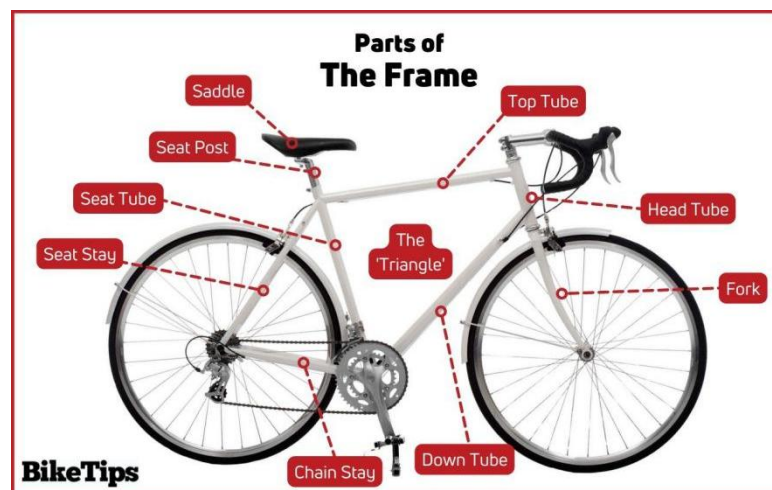


Figure 1.8 Main components of a bicycle[16]

1.2.2 Bicycle chain transmission

The power transmission system of a bicycle is essentially a conversion system, which converts and transmits the force exerted by a person on the bicycle's pedals to the rear wheel of the bicycle, thereby propelling it forward. Single-speed transmission systems are typically used in classic bicycles, recreational bicycles and track bicycles. As shown in Figure 1.9, this transmission system consists of a sprocket and a flywheel connected by a chain. Since the number of teeth on the sprocket is fixed, the transmission ratio cannot change, achieving a fixed transmission efficiency[17]. Since sprocket switching cannot be carried out, multiple transmission ratios cannot be achieved, which may limit performance in certain situations (such as climbing slopes and high-speed driving). However, single-speed transmission systems have the advantages of low cost, light weight, low maintenance cost and high overall reliability.[18]



Figure 1.9 Single-speed Drivetrains[33]

The drive system of a bicycle is based on the traditional sprocket -chain-sprocket system. To operate it, the cyclist must exert a force on the pedal in the direction of movement, rotating the sprocket clockwise if using a Cartesian coordinate system and assuming that the bicycle's displacement is in the direction of the positive X-axis. The main purpose of this article is to study the transmission system composed of sprocket - chain - sprocket

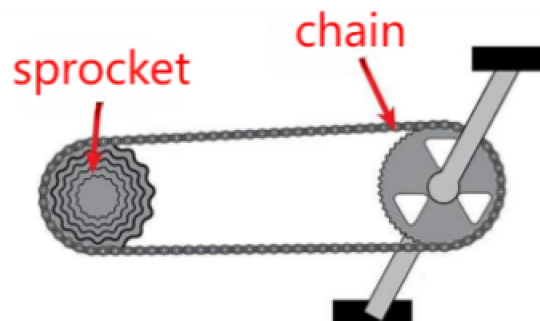


Figure1.10 Chain drive system

A typical roller chain drive system consists of components such as crank arms, pedals, bottom brackets, sprockets, chains, gears or flywheels. A closed-loop roller chain is composed of a series of interconnected rollers and pins [19]. When the drive sprocket rotates, the chain is driven, which in turn drives the driven sprocket to rotate and transmits power from the transmission shaft to the driven shaft [20]. If operated properly, a typical roller chain drive system can achieve an efficiency of 97% to 99%. Figure 1.11 shows the common components or features of a bicycle drive system.

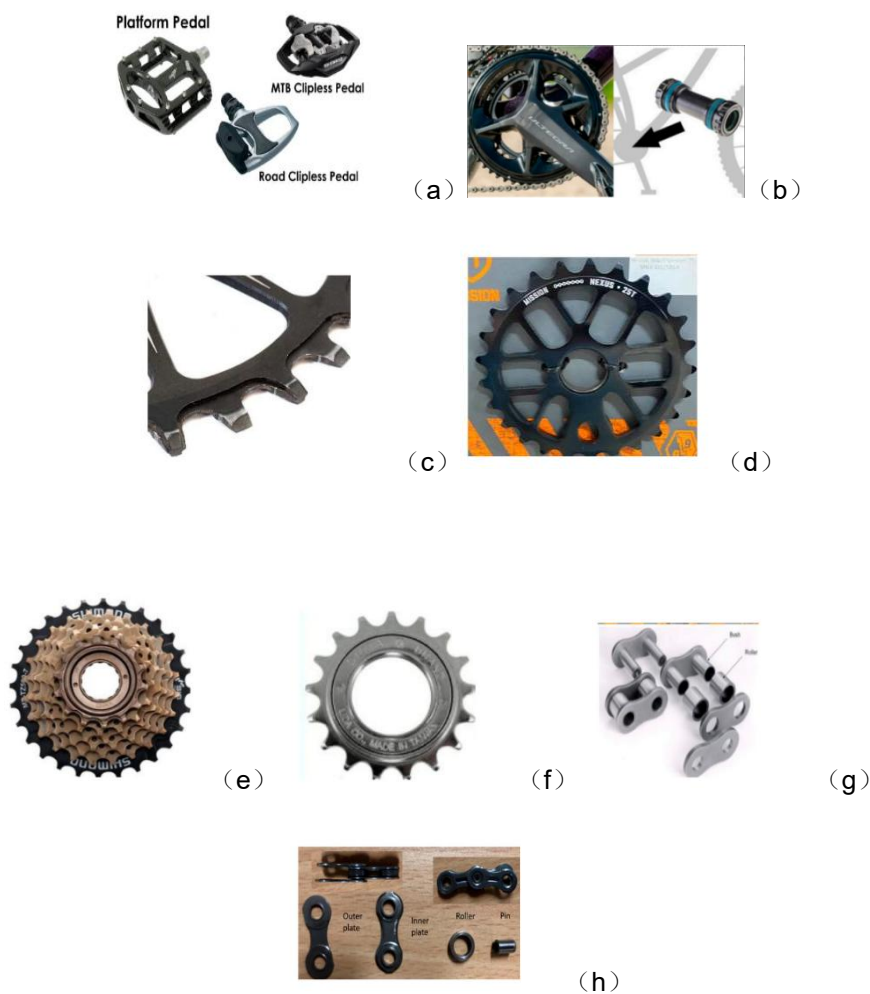


Figure 1.11 Components of the roller chain drive in a bicycle drivetrain system. (a) Pedal; (b) Crank arm and bottom bracket; (c) Wide-narrow chainring - single-speed/1× drivetrain system; (d) Uniform chainring - multi-speed transmission system; (e) Sprocket/gear - single-speed transmission system; (f) Cassette - multi-speed transmission system; (g) Bushed roller chain - single-speed transmission system; (h) Non-bushed chain - multi-speed transmission system.[34]

1.2.3 Crank and sprocket

The bicycle crankset converts the reciprocating motion of the rider's legs into rotational motion, driving the sprockets and chain to transmit power. It consists of several components, including crank arms, pedals, bottom bracket or axle, and bearings, as shown in Figure 1.11.

A sprocket is a toothed, wheel-like component that meshes with the chain to achieve motion and power transmission. Sprockets can be divided into front sprockets and rear cassettes (or cassettes on multi-speed bicycles), as shown in Figures 1.11-c-f. The toothed ring connecting the bicycle crank is called a sprocket. Bicycles have one, two, or three front sprockets/chainrings; the larger the sprocket, the harder it is to pedal; the smaller the sprocket, the easier it is to pedal. Sprockets come in various sizes and shapes, with the number of teeth ranging from 20 to 53. Sprocket teeth are usually evenly distributed, but some sprockets use a wide-narrow tooth design[21], containing two sets of teeth of different thicknesses. This design ensures better meshing between the chain and the sprocket, preventing the chain from slipping off during riding. Some sprockets even feature optional hook-like structures on the rear side, to better guide the chain. [22]Wide and narrow toothed sprockets are commonly used in fixed-gear and single-speed bicycle drivetrains. In addition, there are some special designs, such as oval sprockets or compact sprockets.

The driven sprocket in a bicycle drivetrain is usually mounted on the rear wheel; it rotates or propels the bicycle forward when the chain drives. The sprocket on the rear wheel hub, individually called a "gear" or "sprocket," is called a "freewheel" when put together. The size of the rear sprocket is opposite to that of the front sprocket—the larger the rear sprocket, the easier it is to pedal; the smaller the rear sprocket, the more difficult it is to pedal (Figure 1.11-f). Most modern road bikes have 8 to 11 gears on their rear freewheel, described by the number of teeth on their rings; for example, "11-speed 10/28" means there are 11 rear sprockets making up the freewheel, with the smallest ring having 10 teeth and the largest having 28 teeth. The number of different gear combinations on a bicycle. In reality, there is often overlap between different gears. For example, a 50/32 and a 34/22 have the same gear ratio (approximately 1.56). Although the gear ratio is the same, the riding feel is completely different.

1.2.4 Chain Drive Assembly

Chain drives are meshing transmissions with a flexible intermediate component, combining some characteristics of gear drives and belt drives. Chain drives are widely used in mechanical transmissions, with chain speeds reaching 40 m/s, power transmission up to 3600 kW, and transmission ratios up to 15. The typical operating range is: power transmission not exceeding 100 kW, chain speed not exceeding 15 m/s, and transmission ratio not exceeding 8.

Compared to belt drives, chain drives have the following advantages: no elastic slippage, accurate average transmission ratio, and slightly higher transmission efficiency; lower tension, resulting in less load on shafts and bearings; and a compact structure, transmitting the same power with smaller overall dimensions than belt drives.

Compared to gear drives, chain drives have the following advantages: larger center distances and lighter structure; ability to operate under harsh conditions (less affected by climate changes); and lower cost.

The disadvantages of chain drives are: higher price and heavier weight than belt drives; chain speed fluctuates and cannot maintain a constant instantaneous transmission ratio; it is noisy during operation and is prone to generating large tension and impact loads at high speeds; it is not suitable for applications where space is limited and the center distance is small or the direction of rotation changes frequently; the chain links become unstable after elongation and are prone to skipping teeth; it can only be used for transmission between parallel shafts.

Numerous studies have explored the setup and configuration of chain drives. Researchers have investigated the optimal gear ratios for multi-speed bicycles, proposing that reducing the number of gears without compromising physiological efficiency can make shifting easier, as a smaller number of optimal gears can provide performance comparable to a multi-speed system.[23] This reduces the overall mass of the transmission system and achieves optimal functionality.

Some studies have investigated the impact of bicycle sprocket shape and geometry on overall performance, focusing on non-circular sprockets and developing algorithms and models that represent gear ratios using crank angle and effective radius functions.[24] Their findings indicate that sprocket shape has no significant impact on overall transmission efficiency. Due to technological advancements and innovations, computer-aided engineering (CAE) tools and techniques have been applied to the analysis and optimization of chain drive geometry; for example, 3D modeling of roller chain drives allows for finite element static and dynamic analysis, as well as topology optimization.[25]

1.2.5 Research Status of New Bicycle Transmission Mechanisms

The transmission mechanism of a bicycle is the core driving component of the bicycle, and its structure directly affects the riding effect of the bicycle. In order to meet the different needs of bicycle use, new transmission mechanisms are constantly being innovated, which constantly affects the development of bicycles.

The new bicycle launched by the American company TREK [26], as shown in Figure 1.12, abandons the traditional chain drive and innovatively uses a

synchronous belt drive system. Compared with the chain drive of ordinary bicycles, the synchronous belt drive system makes the bicycle not only quieter and lighter, but also less prone to "chain slippage". In addition, the synchronous belt drive does not require the use of lubricating oil, making the bicycle cleaner. However, the bicycle is equipped with the new technology of synchronous belt drive system, and its price is more expensive than that of ordinary bicycles.



Figure 1.12 New Bicycle from TREK Company[26]

CeramicSpeed collaborated with the Department of Mechanical Engineering at the University of Colorado to innovatively design a bicycle drivetrain as an axle-driven shifting system, winning the 2018 Eurobike Award, as shown in Figure 1.13.[27] The rear 13-speed cassette, circular carbon fiber shaft, and chainring serve as the core transmission components. Ceramic balls at both ends significantly enhance rotational speed, substantially improving the bicycle's power performance. Furthermore, this transmission system incorporates principles of physics and aerodynamics, drastically reducing friction resistance and energy consumption. Transmission efficiency reaches up to 99%.



Figure 1.13 Bicycle Shaft Drive Transmission System[27]

American designers Rodger Parker and others developed a chainless bicycle. The pedals generate driving force through a crank-rocker mechanism, propelling the bicycle by pedaling two pedals connected to the rear wheel. In terms of design, the designers employed a crank-rocker mechanism to enhance driving force and extended the crank length, making cycling more effortless. Unlike conventional bicycles where riders' ankles and knees move in a circular motion, the chainless bicycle employs an up-and-down motion for these joints. This design offers some degree of knee protection for the rider.

Austrian company GRUBER Drive Components has developed an innovative bottom bracket drive assist mechanism.[28] Positioned within the seat tube of mountain bikes, this system incorporates a unique spring device between the crankset and chainring. Primarily designed to provide additional propulsive force to the crankset rotation, it significantly increases the bicycle's driving power.

The American company ElliptiGO ingeniously combines bicycles and elliptical machines to achieve better fitness results.[30] It does not use chain drive but pedal drive. Make it better imitate the effect of the indoor elliptical machine. Even more interesting is another innovative hybrid fitness and transportation equipment that ingeniously combines the functional features of traditional bicycles and rowing machines. Rowing bikes feature a unique swing lever power transmission system and are promoted as providing full-body exercise through rowing movements. As the system does not bear weight, it is very gentle on the rider's knees, hips and back. Make it achieve the effect of light burden fitness.[31]



Figure 1.14 ElliptiGO [30]



Figure 1.15 Rowbike [31]

2 Design the chain transmission connection

2.1 Basic Introduction to Roller Chains

A roller chain consists of 1. Outer plate, 2. Inner plate, 3. Pin, 4. Bushing, 5. Roller. The inner chain plates and bushings, and the outer chain plates and pins, are fixed together by interference fits. The rollers and bushings, and the bushings and pins, are clearance fits. When the inner and outer chain plates flex relative to each other, the bushing can rotate freely around the pin. The rollers are loosely fitted onto the bushings; during operation, the rollers roll along the sprocket tooth profile, reducing tooth wear. Chain wear mainly occurs on the contact surface between the pin and bushing. Therefore, a small gap should be left between the inner and outer chain plates to allow lubricating oil to penetrate between the friction surfaces of the pin and bushing. The inner and outer chain plates are made in a figure-eight shape to ensure that each cross-section of the chain has similar tensile strength, and also to reduce the chain's mass and inertial forces during movement.

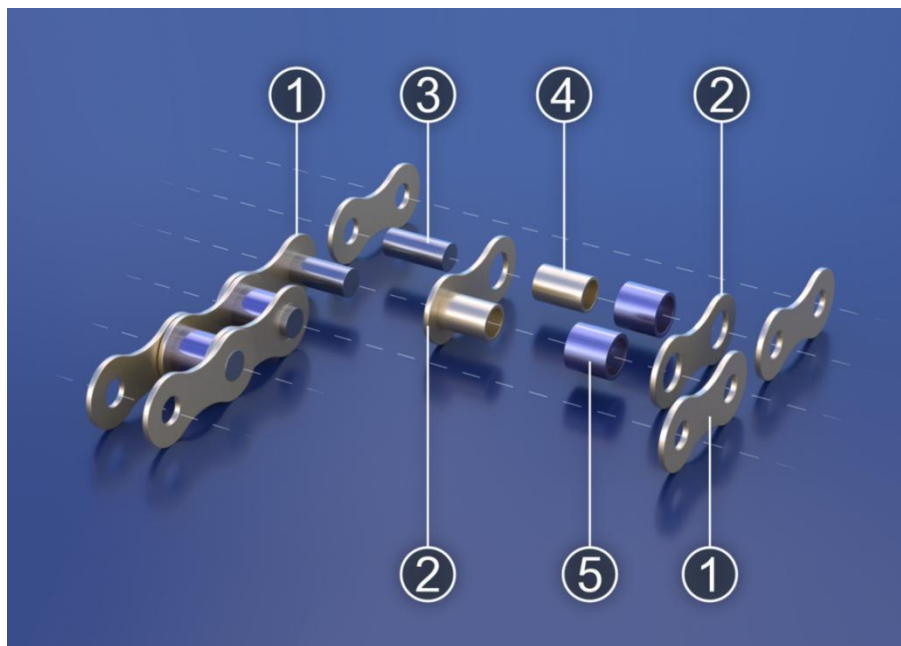


Figure 2.1 Roller chain composition[29]

When using a drive chain, the two ends are connected in a loop. When the number of links is even, the joint can be secured by overlapping inner and outer chain plates, and then locked with cotter pins or spring clips. If the number of links is odd, a transition link is required to connect the two ends. When the chain is under tension, the transition link will be subjected to an additional bending

moment, so chains with an even number of links should be used whenever possible.

The basic parameters for the meshing of a roller chain and sprocket are the pitch p , the outer diameter d_1 of the roller, and the inner width b_1 of the inner link. Among these, the pitch is the most important parameter of the roller chain. As the pitch increases, the dimensions of each component in the chain must also increase accordingly, and the power that can be transmitted also increases. However, when the number of sprocket teeth is constant, the larger the pitch, the larger the sprocket diameter D . To prevent D from becoming too large, double-row or multi-row chains with a small pitch can be used when the load is large. The load-bearing capacity of a multi-row chain is directly proportional to the number of rows; the more rows, the higher the load-bearing capacity. However, due to manufacturing and installation errors, it is difficult to make the load on each row uniform. The more rows there are, the more serious the unevenness becomes. Therefore, the number of rows should not be too many, generally not exceeding four rows.

2.2 Chain selection

In the design of roller chain drives, the commonly known raw data typically include: power, drive shaft speed, transmission ratio, basic center distance requirements, and environmental conditions. Chain drive design calculations primarily determine suitable transmission parameters through experimental methods and by consulting graphical data. The following is general steps in the calculation of roller chain drive design.

Determine the number of sprocket teeth. The number of sprocket teeth has a significant impact on the smoothness and service life of the chain drive. The number of teeth on the smaller sprocket should be selected based on the chain speed. Generally, the number of chain links is an even number; therefore, the number of sprocket teeth should be an odd number that is coprime to the number of chain links, which is beneficial for even wear. The selection of the number of teeth z_2 on the smaller sprocket is shown in Table 1, and the number of teeth on the larger sprocket is $z_1 = z_2 i$. Here, z_2 is set to 16.

Table 1 Tooth number of the small sprocket

Chain speed v [m/s]	0.6~3	3~8	>8
z_2	$\geq 15 \sim 17$	$\geq 19 \sim 21$	$> 23 \sim 25$

Next, we need to determine the chain type and pitch. Figure 2.2 shows a typical rated power curve for a single-row roller chain. Based on the rated power and the speed of the drive sprocket, the appropriate chain type can be easily selected. Here, we use this example for modeling: with the rider weighs 60kg and pedals at a speed of $n_1 = 40$ r/min; the bicycle weighs approximately 10kg, the tire

diameter is approximately 0.66m, and the riding speed is 12km/h, approximately 3.3m/s.

Select the number of sprocket teeth. Take the number of teeth on the small sprocket as $z_2=16$.

$$v_{bike} = \frac{\pi d_{wheel} n_2}{60} \quad (1)$$

$$n_2 = \frac{60 v_{bike}}{\pi d_{wheel}} = 95.5 \approx 96 \text{ r/min} \quad (2)$$

$$i = \frac{n_1}{n_2} = \frac{40}{96} = 0.4167 \approx 0.42 \quad (3)$$

$$z_1 = \frac{z_2}{i} = 35.7 \approx 38 \quad (4)$$

Determine the calculated power

$$F_N = (m_{human\ mass} + m_{bike\ mass})g = (60 + 10) \times 10 = 700 \text{ N} \quad (5)$$

$$F_f = f F_N = 0.7 \times 700 = 490 \text{ N} \quad (6)$$

Note: The coefficient of friction between the tire and the ground is $f = 0.7 \sim 0.8$.

$$P = F_f v = 490 \times 3.3 = 1617 \text{ W} = 1.617 \text{ kW} \quad (7)$$

Given $K_A = 1.0$ (This is a stable load operating condition.) and $K_Z = 0.49$, and a single-row chain, the calculated power is:

$$P_{ca} = K_A K_Z P = 1.0 \times 0.49 \times 1.617 = 0.79 \text{ kW} \quad (8)$$

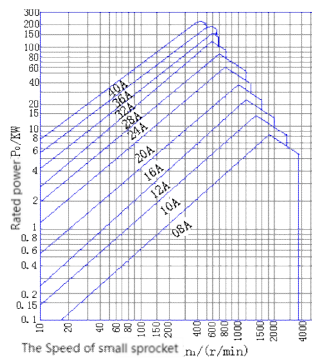


Figure 2.2 Rated power curve of a single-row roller chain[32]

Based on $P_{ca}=0.79\text{kw}$ and $n_1=40\text{r/min}$, the chain model can be taken as 12A-1, therefore the pitch $p=19.05\text{mm}$.

In design, the center distance is generally taken as $a_0 = (30\sim 50)p$, and the maximum is taken as $a_{0\text{max}} = 80p$.

$$a_0 = (30 \sim 50) \times p = (30\sim 50) \times 19.05 = 571.5\sim 952.5\text{mm} \quad (9)$$

Here, a_0 is taken as 600mm.

$$L_p = \frac{2a_0}{p} + \frac{z_1 + z_2}{2} + \left(\frac{z_2 - z_1}{2\pi}\right)^2 \frac{p}{a_0} = 90.4 \quad (9)$$

Here, L_p is taken as 90.

The maximum center distance of the chain drive is:

$$a = \frac{p}{4} \left[\left(L_p - \frac{z_1 + z_2}{2} \right) + \sqrt{\left(L_p - \frac{z_1 + z_2}{2} \right)^2 - 8 \left(\frac{z_2 - z_1}{2\pi} \right)^2} \right] = 596\text{mm} \quad (10)$$

Calculate chain speed v_c and determine lubrication method.

$$v_c = \frac{n_1 z_1 p}{60 \times 1000} = 0.4826 \text{ m/s} \quad (11)$$

Based on $v_c=0.4826 \text{ m/s}$ and the chain number, regular manual lubrication should be used.

Effective circumferential force F_e

$$F_e = \frac{1000P}{v_c} = 3351 \text{ N} \quad (12)$$

The axial force coefficient K_{FP} when the sprockets are arranged horizontally is 1.15.

$$F_p = F_e \times K_{FP} = 3853 \text{ N} \quad (13)$$

2.3 Roller chain modeling and assembly

SolidWorks is a user-friendly and highly efficient 3D mechanical design software that integrates core functions such as 3D modeling and assembly design. Without the need for complex programming, it can precisely create models of mechanical components, making it an important digital tool for enhancing competitiveness in the industrial sector.

The roller chain, as a commonly used mechanical transmission component, has achieved standardization in its structure. The key parameters can be found in the GB/T 1243-2024 "Roller Chains and Sleeve Chains" standard, providing a unified basis for three-dimensional design and ensuring the universality and interchangeability of the design.

When designing a roller chain using SolidWorks, for the core components such as the inner and outer link plates and pins, a simplified modeling method can be adopted, dividing them into two parts: the inner part (the parts subjected to force and in close contact) is modeled precisely according to standards, while the outer part (the non-critical structure) can be appropriately simplified. The modeling can refer to the extrusion and arrangement methods shown in Figures 2.3 and 2.4. Plate-type parts are formed through extrusion and chamfering features, and shaft-type parts are rapidly formed through rotational extrusion and other methods, balancing accuracy and efficiency.

The three-dimensional design of roller chains mainly includes chain body modeling and component modeling: Chain body modeling completes the construction of individual components to ensure dimensional accuracy; Component modeling precisely assembles according to the actual assembly relationship, adds fit constraints and checks for interference to ensure the reliability of the transmission. In addition, by leveraging the parametric function of SolidWorks, standard parameters can be associated to quickly generate models of roller chains of different specifications, thereby enhancing the efficiency of batch design.

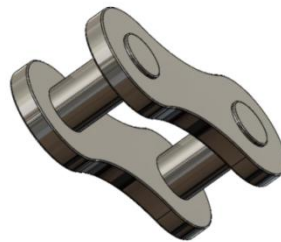


Figure 2.3 Outer chain

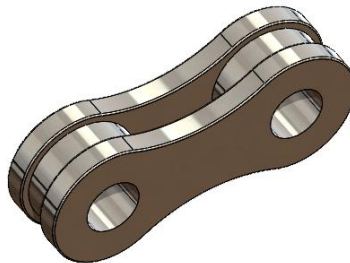


Figure 2.4 Inner chain

After importing the parts, the key step is to use the mating commands in SolidWorks for precise assembly. According to the mating requirements of different components, select the appropriate mating type: for the mating parts such as pins and sleeves, or sleeves and rollers that need to rotate coaxially, use the coaxial mating command to ensure that the axes of all components are completely coincident, ensuring smooth rotation; for fixed connection parts such as inner chain plates and sleeves, or outer chain plates and pins, use the face coincidence mating command to make the connection surfaces of the components closely adhere, determining the relative position; if there is an unreasonable mating gap, add the distance constraint command to fine-tune the gap to ensure that the components are closely connected without any sticking.



Figure 2.5 Roller chain assembly



Figure 2.6 Chain drive assembly drawing

3 Design CAM for the front sprocket

3.1 Model Preprocessing and CAM Environment Construction

3.1.1 Model Preprocessing

Bicycle sprockets are thin-disc toothed transmission parts, and their machining accuracy directly affects transmission smoothness and service life. Therefore, the completed CAD model needs to undergo pre-verification and preprocessing: Verify the geometric integrity of the model, ensuring that core features such as sprocket teeth, mounting bores, keyways, and axial dimensions are intact. The model should be a closed, unbroken solid structure without geometric interference or redundant surfaces. Standardize the model unit to metric millimeters (mm), ensuring that dimensional and geometric tolerances conform to relevant machining standards, achieving consistency between design and subsequent process datums. Remove decorative and auxiliary features unrelated to machining from the model, simplifying the CAM calculation process and avoiding interference from non-machining features in toolpath generation.

3.1.2 CAM environment setup

Processing Coordinate System (WCS) setup

Origin positioning: The WCS origin is set at the rotation center of the top surface of the chain wheel blank, which is exactly coincident with the design reference of the chain wheel; the positive direction of the Z-axis is perpendicular to the top surface and points upward, while the X/Y axes are aligned with the machine coordinate system.

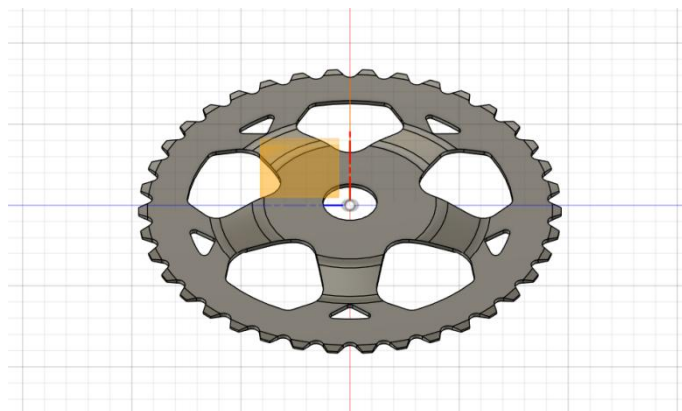


Figure 3.1 WCS coordinate setting

During the setup of the Fusion 360 machining module, the system generates a blank based on the center position of the model, using relative tetrahedral dimensions. The system automatically generates a tetrahedral blank with a complete contour coating to adapt to the cutting process, compensate for the size and shape deviations of the raw material, reserve uniform and sufficient machining allowance for subsequent milling processes, and ensure that cutting operations can be performed throughout the entire machining area.

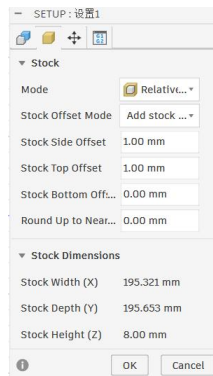


Figure 3.2 Setting of cylindrical material blanks

3.2 Machine tool model selection

Given the structural characteristics of the bicycle chain wheel and the strict requirements for CNC machining, in the Fusion 360 simulation environment, after comprehensive consideration and comparative analysis, we finally chose a three-axis vertical machining center with a main spindle that can move along the Z-axis. This equipment selection was not made arbitrarily but was determined based on factors such as the processing requirements of the chain wheel, equipment performance, simulation effect, and engineering economy. Its rationality and necessity mainly lie in the following five aspects, fully meeting the core demands of chain wheel CNC machining.

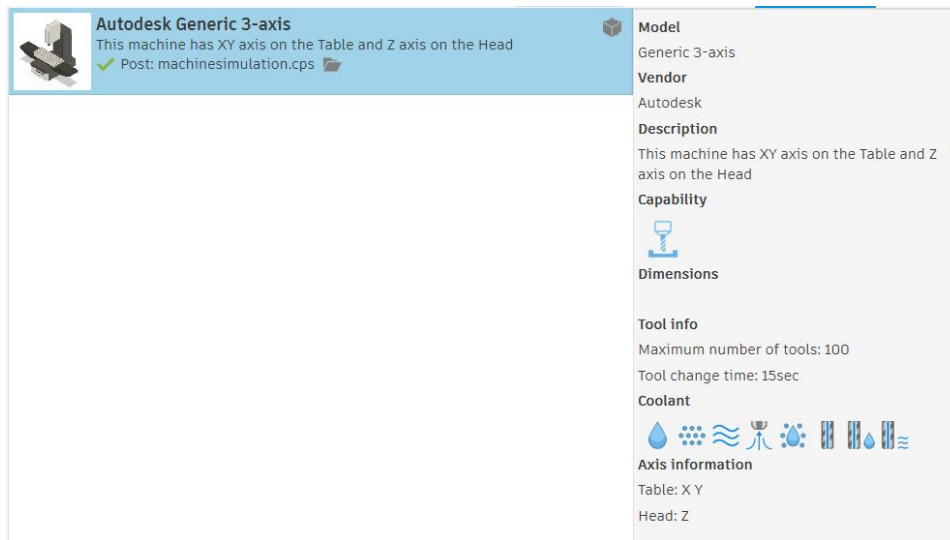
Firstly, this structure has extremely strong processing adaptability and can precisely match the processing requirements of the bicycle chain wheel. The bicycle chain wheel, as a typical disc-shaped rotating component, has clear processing contents, mainly including external contour milling, precise processing of tooth shapes, center hole drilling and fine processing, as well as end face slot milling, all of which belong to planar processing and two-dimensional contour processing, and do not require complex multi-axis linkage actions. The vertical main spindle of the three-axis vertical machining center is arranged along the Z-axis perpendicularly, which can directly achieve X, Y, and Z three-axis linkage control, covering the milling range of all processing procedures of the chain wheel, without the need for more costly and more complex multi-axis processing equipment, and the process route is simple, clear, and reliable, avoiding the

problem of redundant processes and increased operational difficulty caused by multi-axis equipment.

Secondly, this processing equipment is technologically mature and has high operational stability, ensuring the accuracy of chain wheel processing. The Z-axis vertical milling machine is one of the most widely used and technologically mature equipment types in the mechanical processing field. After long-term engineering practice verification, its structure design is reasonable, the clamping method is convenient, and the positioning accuracy can meet the strict standards for chain wheel processing. Its vertical spindle structure is more conducive to the positioning and clamping of the workpiece, facilitating the realization of a unified processing benchmark, effectively avoiding processing defects caused by positioning deviations, precisely ensuring the tooth pitch accuracy, tooth profile consistency, concentricity of the center hole, and flatness of the end face, fully meeting the dimensional tolerances and position tolerances required for the chain wheel as a transmission component, providing a solid guarantee for processing quality.

Furthermore, this equipment is compatible with the Fusion 360 simulation environment, has strong stability, and is convenient for the verification and optimization of processing programs. In the Fusion 360 CAM simulation scenario, the model library resources of the Z-axis vertical machine tool are rich, and its compatibility with the software is extremely high, supporting complete tool path simulation, overcut checking, and collision detection between the equipment and the workpiece, as well as between the tool and the workpiece. Compared with other types of machines, this vertical structure machine has a simple and clear motion logic, stable and reliable simulation process, and can precisely reproduce every step of actual processing, promptly detecting unreasonable parts of the program, deviations in the tool path, and potential collision risks, providing effective simulation verification for the generation, optimization of CNC codes, and safety of the processing process, reducing the occurrence rate of faults in actual processing.

Finally, this equipment has significant cost and efficiency advantages, conforming to engineering practice and economic principles. Compared with horizontal machining centers or multi-axis machining machines, the equipment purchase cost, maintenance cost of the three-axis vertical machining center are lower, and the processing efficiency is higher, the operation process is simpler, and the skill requirements for operators are relatively mild. Under the premise of ensuring that the processing quality of the bicycle chain wheel meets the standards, choosing this equipment can effectively simplify the processing process, shorten the processing cycle, and reduce the overall manufacturing cost, not only meeting the technical requirements of chain wheel processing, but also conforming to the economic principles in engineering practice, achieving dual guarantees of quality and efficiency.



Autodesk Generic 3-axis
This machine has XY axis on the Table and Z axis on the Head
✓ Post: machinesimulation.cps

Model
Generic 3-axis

Vendor
Autodesk

Description
This machine has XY axis on the Table and Z axis on the Head

Capability

Dimensions

Tool info
Maximum number of tools: 100
Tool change time: 15sec

Coolant

Axis information
Table: X Y
Head: Z

Figure 3.3 Machine tool model

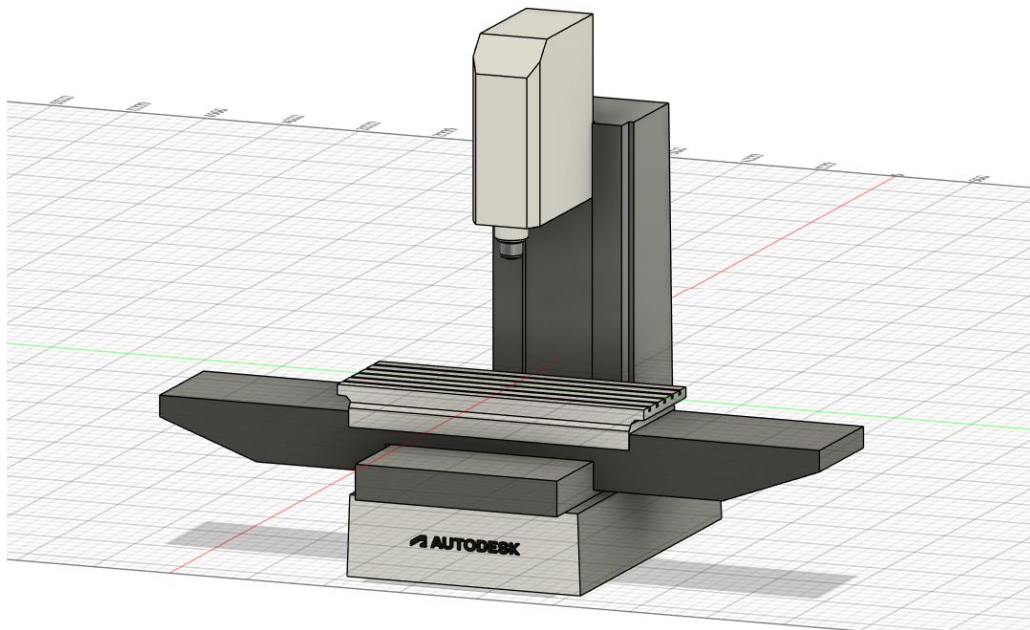


Figure 3.4 Three-axis machine tool 3D model

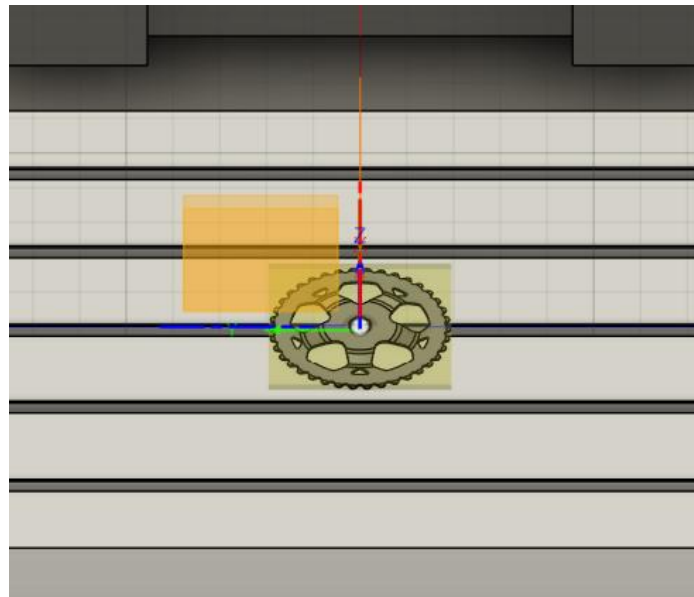


Figure 3.5 The parts are set up on the machine tool.

- Since the three-axis machine used can only perform milling on the z-axis, the principle of double-sided processing is adopted, with the first side being processed and then the semi-finished blank being removed before processing the other side. Although this process is laborious, the cost of the machine used is low, which can effectively reduce the production cost.

Table 2. List of Tools

Process type	Type of tools	Core parameters
Rough process	4-blade hard alloy flat-head face milling cutter	50mm Face Mill
Finishing process	3-bladed hard alloy flat-head milling cutter	10mm Flat Endmill
Finishing process	3-blade hard alloy ball-end milling cutter	5mm Ball Endmill
Finishing process	3-bladed hard alloy flat-head milling cutter	6mm Flat Endmill

3.3 Simulation settings

First, perform rough processing: clean the two-dimensional surface. Click on the "2D - Face Milling" option in the top menu bar to open the tool path settings window. Select a 50-millimeter face milling cutter, select the surface area of the workpiece, and process the surface; set the cutting parameters to spindle speed of 5000 revolutions per minute and cutting feed speed of 1000 millimeters per minute, optimize the idle path to reduce non-cutting time. After confirming there are no errors, generate the rough processing tool path.

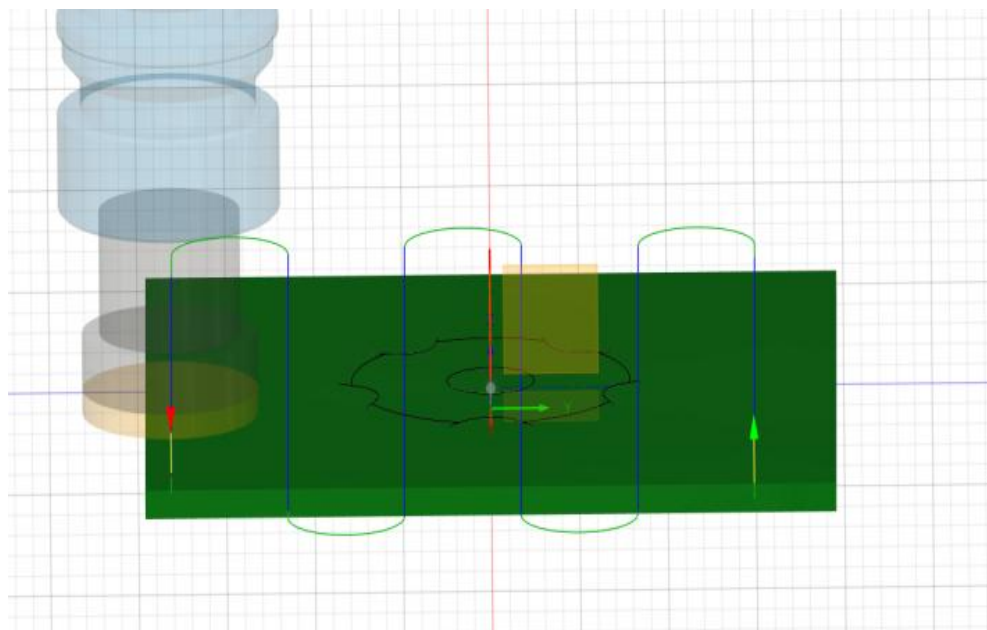


Figure 3.6 Face milling cutter path

After completing the initial model positioning and parameter presetting, a rough processing operation needs to be carried out using the adaptive cleaning tool. First, in the top menu bar of the software, find the "3D" option and click on it. In the pop-up drop-down menu, precisely select "Adaptive Cleaning Tool", and after clicking, the tool path setting window will be opened. In the tool selection column of the window, filter and select the flat-end milling cutter with a specification of 10 millimeters. This cutter has moderate rigidity and high cutting efficiency, and is suitable for the requirement of removing a large amount of excess materials in the rough processing of the gear chain. After confirming that the tool selection is correct, in the processing area settings, select the entire core processing area of the gear chain to be processed, and check the "Full Area Coverage" option to ensure no processing omissions. After clicking "Confirm Processing", the equipment will automatically run according to the preset path.

This rough processing procedure can efficiently remove 80% of the excess materials on the surface and inside of the gear chain. After processing, the tooth shape, hole diameter, and pitch of the sprocket will be clearly visible, laying a solid foundation for the subsequent fine processing procedures and effectively improving the subsequent processing accuracy and efficiency.

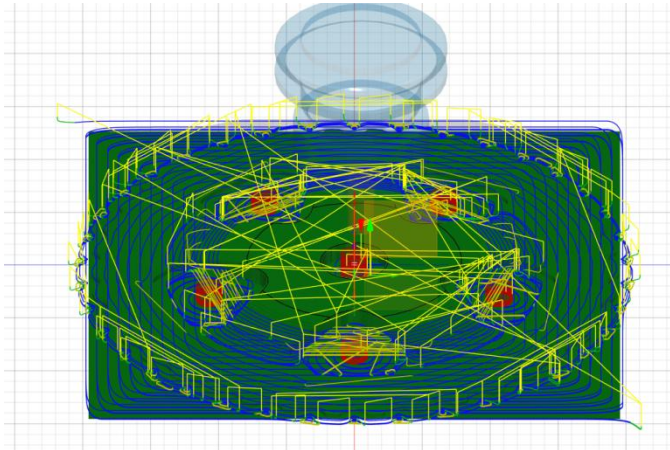


Figure 3.7 3D adaptive path clearing tool path

After the rough processing is completed, the fine processing procedure needs to be carried out immediately on the end face of the sprocket. This is a crucial step to ensure the subsequent assembly accuracy and stability of the sprocket. The core objective is to ensure that the surface finish and dimensional accuracy of the sprocket fully comply with the design standards, laying a solid foundation for subsequent assembly operations and long-term use. During the specific operation process, the parallel milling process is given priority to precisely process the upper end face of the sprocket. Before the operation, the milling speed and feed rate need to be precisely adjusted according to the material and size parameters of the sprocket to ensure a reasonable match between them. At the same time, the cutting path must be strictly controlled to ensure uniform and orderly cutting without any deviation, and any improper operation must be strictly avoided to prevent scratches, unevenness or dimensional deviations on the sprocket surface, which may affect the subsequent usage effect.

At the same time, the bending area on the sprocket needs to be carefully cleaned. This area is prone to residual burrs and excess debris. If not thoroughly removed, it will cause the contour of the sprocket to be irregular, thereby affecting the assembly fit. During the cleaning process, special tools should be used to check the bending area point by point, precisely removing all residual burrs and debris to ensure that the contour of the sprocket is smooth and regular, without any protrusions or depressions. Due to the extremely high precision requirements of the fine processing, conventional milling tools cannot meet the processing needs of the fine contour. Therefore, a 5-millimeter ball-end milling cutter is selected here. Its cutter head is smooth and round, and the cutting process is stable, which can effectively reduce the damage to the sprocket surface during the cutting process, better adapt to the fine contour of the sprocket upper surface, and precisely complete the surface grinding and forming operations.

Through the above fine processing procedures, the upper surface of the sprocket finally reaches the required surface finish and flatness. This not only ensures the sealingity and stability of the subsequent assembly process, avoiding faults caused by excessive assembly clearance or poor fit, but also effectively improves the precision and efficiency of subsequent

processing procedures, ensuring the overall processing quality of the sprocket and extending its service life.

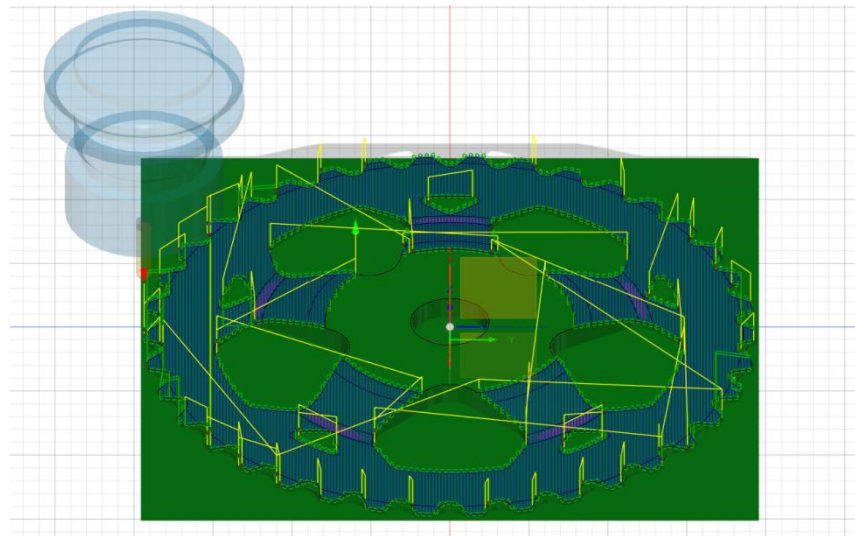


Figure 3.8 Parallel processing path

After the main area of the sprocket has been processed, the teeth of the sprocket are processed. Here, we adopt 2D processing and technology. This not only thoroughly processes the teeth of the sprocket, but also removes the excess parts of the blank.



Figure 3.9 The path for processing the teeth of the sprocket

For this side chain wheel, after completing the preliminary rough machining and semi-finish milling forming and other preparatory processes, the next step will be the full-process final precision machining stage. To meet the core

requirements of precise positioning for subsequent shaft assembly and key connection, we will use high-precision CNC equipment to perform standardized slotting processing on the main holes such as the installation reference holes and transmission positioning holes on the chain wheel. During the processing, the size tolerance, shape accuracy and surface roughness of the slot type will be strictly controlled to ensure that the holes after slotting can achieve precise and gap-free adhesion with the matching components. At the same time, it will significantly enhance the torsional bearing capacity and operational stability of the chain wheel during transmission, providing core process guarantee for the final quality and long-term service life of the finished chain wheel.

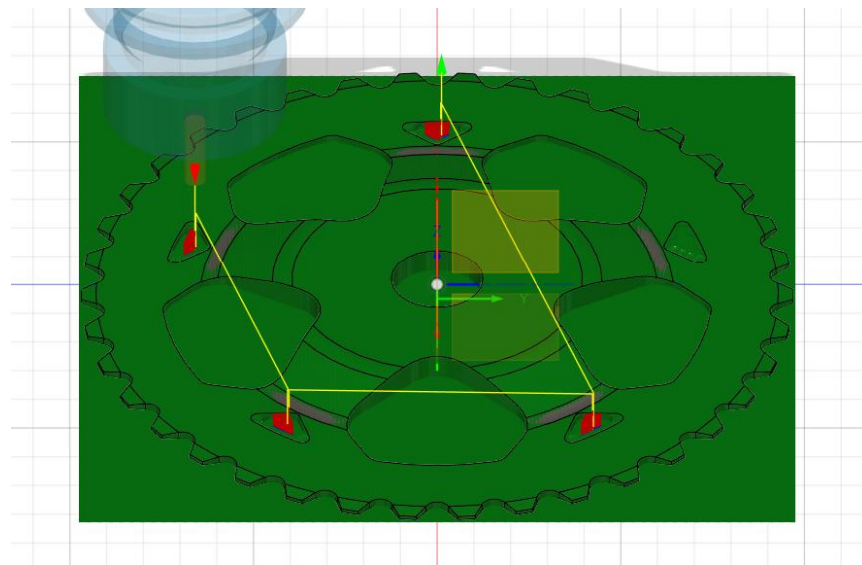


Figure 3.10 Slotting path

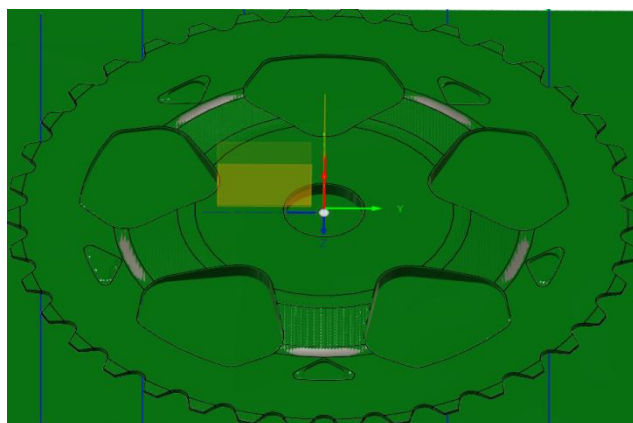


Figure 3.11 Initial treatment outcome

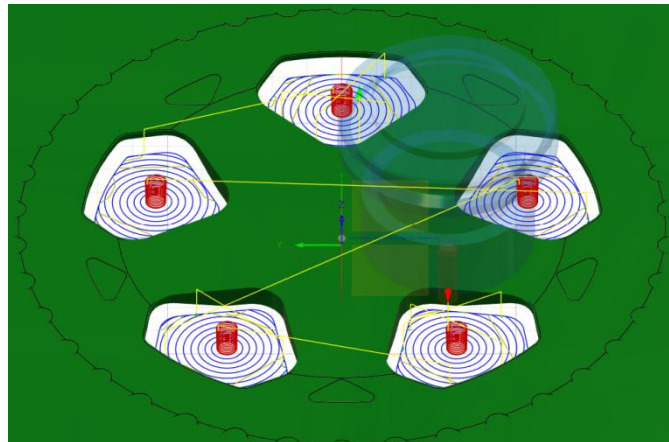


Figure 3.13 Slotting processing path

After the slotting process is completed, the final step requires meticulous processing. This involves carefully polishing the surface of the chain wheel to completely remove any burrs, scratches and excess materials generated during the manufacturing process. The aim is to ensure that the surface is smooth and flat, and the dimensions are accurate without any errors. Eventually, a finished chain wheel that meets the design standards and can be put into practical use is formed.

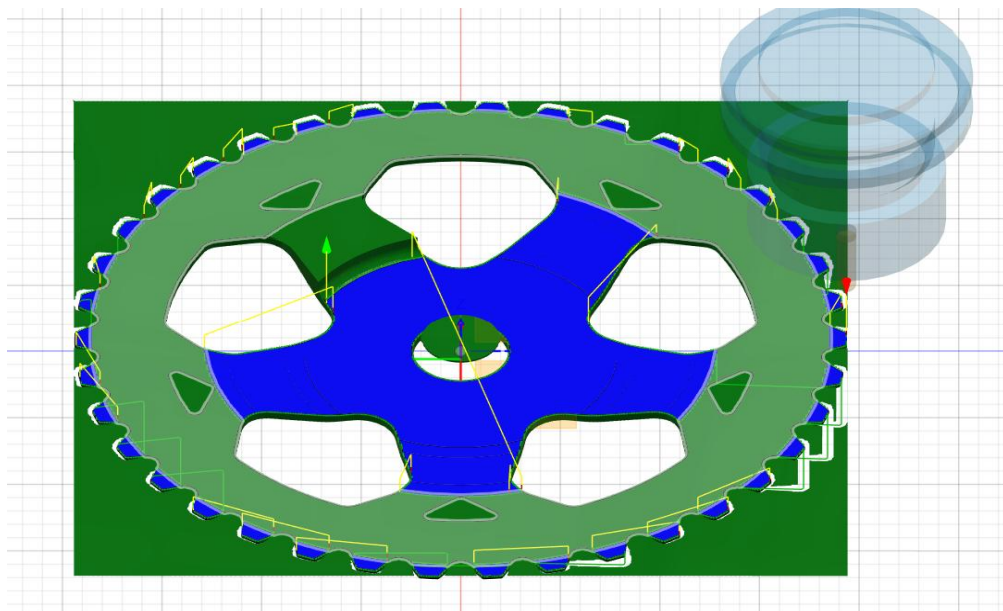


Figure 3.14 Removal processing path

After completing the design of the complete tool path for the entire processing procedure, the subsequent operations must be carried out strictly in accordance

with the prescribed steps to ensure the smooth progress of the subsequent processing simulation. First, the operator needs to precisely select all the planned tool paths in the design interface. This can be done by holding down the shortcut key to select them in batches to ensure that no paths are missed or selected incorrectly, and to avoid generating incomplete results due to some paths not being selected. After selection, click the "Operation - Generate" option in the top menu bar. At this point, the system will automatically start the calculation program for the tool path trajectory. Be patient while waiting for the calculation to complete. During this period, do not interrupt the operation or close the software randomly to prevent calculation errors.

After the calculation is completed, carefully check the feedback information on the interface. Focus on confirming that there are no red error messages in the bottom information bar. At the same time, check the tool path trajectory one by one through the preview window to ensure that there are no overlapping paths, breakpoints, exceeding the processing range, or tool interference. This step is crucial. Only after completing a comprehensive verification and ensuring that the tool path design fully meets the processing requirements, can the next stage of machine tool simulation be entered. This can prevent failure of the machine tool simulation due to defects in the tool path (such as incorrect trajectories, interference, etc.) from the very beginning, reduce repetitive operations, improve work efficiency, and also detect potential processing risks in advance to ensure the safety and accuracy of the subsequent actual processing.

After the comprehensive verification of the tool path and the repeated testing of the machine tool simulation, the feasibility of this processing step has been fully proven. It should be noted that the machine used in this simulation is an Autodesk virtual machine tool, whose core function focuses on the simulation verification of the processing process, rather than the export of actual production codes. Therefore, it is impossible to directly export the G-code for actual machine tool processing. However, even so, the manufacturing process can still be fully simulated through this virtual machine tool. Through the simulation, one can visually observe the movement trajectory of the tool, the cutting sequence, the spindle speed, the feed rate, and other key parameters, and restore the real processing scene. This further verifies the rationality of the processing flow and the correctness of the tool path, providing a reliable reference basis for the subsequent actual machine tool processing, and early detection and resolution of possible processing problems to ensure the smooth progress of actual production.

4 Design CAM for the back sprocket

4.1 CAM Environment Construction

4.1.1 CAM environment setup

Regarding the manufacturing simulation process for the rear sprocket, we still use the three-axis machine tool that was uniformly selected in the previous stage for simulation modeling and processing simulation, ensuring that the simulation platform for all series of components, equipment parameters, and computing environment remain consistent. This not only reduces the simulation debugging cost but also guarantees the universality and comparability of the processing data, avoiding deviations in the simulation results due to equipment switching.

However, compared to other similar components, the overall appearance contour, surface distribution, and structural characteristics of the rear sprocket have obvious particularities, which determines that there are significant differences in the entire process steps of simulation manufacturing, process path planning, and cutting instruction selection between them. The original processing simulation scheme cannot be directly copied. From the structural characteristics, the core feature of the rear sprocket is the large number of ring surfaces, complex surface curvature, and dense annular cutting areas. It not only includes the annular curved surfaces of the peripheral meshing gear ring, but also involves concentric ring-shaped structures such as the inner hole positioning ring surface and end face transition ring surface. Moreover, the connection accuracy and surface finish requirements between each ring surface are high, and conventional linear cutting, layer milling, etc. processes cannot meet the processing requirements.

Based on this structural characteristic, in the simulation process of the rear chain wheel manufacturing, the cutting strategy and command calling logic were specifically optimized to significantly increase the usage frequency of the ring cutting and circumferential equidistant cutting commands, thereby meeting the efficient processing requirements for multi-ring surfaces. Among them, the ring cutting command is mainly applied in the rough machining stage of a single circular surface, performing circular cutting around the center of the ring to quickly remove excess raw material and ensure the basic forming accuracy of the ring surface; the circumferential equidistant command is mostly used in semi-finish machining and finish machining stages, making layer-by-layer cutting along the contour of the ring surface, which can not only ensure uniform cutting allowances for each ring surface, but also improve the surface smoothness of the curved surface, avoiding problems such as uneven cutting lines and dimensional deviations, and conforming to the structural processing characteristics of the rear chain wheel, achieving a high degree of matching between simulation processing and actual production.

Before conducting the cutting simulation, it is necessary to complete the configuration of the basic parameters of the simulation environment. The core focuses on the two modules of the workpiece coordinate system (WCS) and the blank model. Based on the motion characteristics of the three-axis machine tool and the structural dimensions of the rear sprocket, the processing reference and the boundary of the blank are precisely defined. This lays a solid foundation for generating subsequent circular cutting, circumferential cutting, and equidistant cutting paths, avoiding problems such as simulation collision with the tool, overcutting, and undercutting due to reference deviation or incorrect blank parameters.

The workpiece coordinate system is the core of the three-axis machine tool simulation positioning. It needs to be specifically calibrated based on the symmetrical ring structure of the rear sprocket to eliminate positioning errors caused by the general coordinate system. First, the center axis of the rear sprocket's hole is used as the Z-axis reference, and the coordinate system origin is set at the intersection point of the sprocket end face and the center hole. This not only conforms to the Z-axis feed direction of the three-axis machine tool but also ensures uniform rotation around the center axis during circular cutting and circumferential equidistant cutting. The X-axis and Y-axis are symmetrically arranged along the radial direction of the sprocket, parallel to the machine tool worktable plane, ensuring the regularity of the radial cutting feed path.

At the same time, the WCS is locked as an absolute coordinate system, prohibiting coordinate system offset and rotation during the simulation. The travel parameters of the machine tool's coordinate axes are simultaneously associated, and the positive and negative limit values of each axis are marked. For multi-ring surface layer cutting scenarios, an auxiliary coordinate system is set for local ring face tool setting, and the auxiliary coordinate system is rigidly associated with the main WCS, meeting the requirements for precise tool setting while not disrupting the overall positioning reference, and ensuring the continuity of the entire cutting path. The blank model needs to conform to the forming process of the rear sprocket and the processing range of the three-axis machine tool, using a relative size cube as the basic blank material.

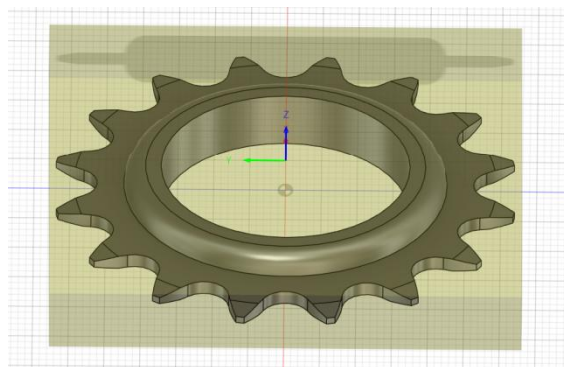


Figure 4.1 WCS and blank setting

4.2 Machine tool model selection

For this simulation, the selected cutting tools were precisely matched based on the motion characteristics of the three-axis machine tool, the requirements for multi-ring surface processing of the rear sprocket, and the characteristics of the cutting process. They also took into account the overall process demands of efficient removal of excess material during rough machining, uniform removal of excess material during semi-finish machining, and maintaining accuracy during finish machining. The tool materials, blade shapes, and specifications were all suitable for circular cutting and equidistant cutting paths, eliminating simulation anomalies such as over-cutting, vibration of the tool, and substandard surface roughness caused by improper tool selection. At the same time, they were in line with actual production tool configurations to ensure that the simulation results can be directly applied in practice.

Table 3. List of Tools

Process type	Type of tools	Core parameters
Rough process	4-blade hard alloy flat-head face milling cutter	50mm Face Mill
Finishing process	3-bladed hard alloy flat-head milling cutter	8mm Flat Endmill
Finishing process	3-bladed hard alloy flat-head milling cutter	3mm Flat Endmill
Finishing process	3-bladed hard alloy ball-head milling cutter	6mm Ball Endmill
Rough process	3-bladed hard alloy flat-head milling cutter	20mm Flat Endmill

4.3 Simulation settings

Based on the structural characteristics of the rear chain wheel, the numerical control processing path is compiled following the principles of regional division, sequential division, and from the outside to the inside. Strictly adhering to the processing guidelines of "priority to positioning reference, separation of rough and fine, and layer-by-layer material removal", the center hole positioning cutting process is carried out first to lay a solid foundation for the subsequent ring cutting. Then, in the order of the outer ring gear ring, end face transition ring, and inner hole positioning ring, layer-by-layer progressive cutting from the outside to the inside is implemented to avoid problems such as ring surface interference and uneven material distribution. During the rough processing stage, the ring cutting

strategy is adopted throughout, with each ring surface's geometric center as the rotation center, and a constant circular path is set. Through layer-by-layer ring cutting, the excess material of the blank is quickly removed, significantly improving the roughing efficiency while ensuring the regularity of the rough machining contour of each ring surface. In the semi-finish and finish processing stages, the strategy of circumferential equal-distance cutting is switched. It conforms to the curvature and contour trend of various ring surfaces, sets uniform step distances and row spacings, and makes equal-spacing layer-by-layer feed along the normal direction of the ring surface. The machining path is finely optimized by refining the turning corner arcs, entering and exiting trajectories, eliminating sudden changes in the machining path, hard cuts at the corners, and messy tool marks. After the complete processing path is generated, the path preview function of the simulation platform is activated to check the tool path section by section. The focus is on checking potential safety hazards such as broken tools, empty tools, and tool interference with the tooling and blank. For unreasonable cutting sections, redundant paths, and interference points, the cutting sequence, cutting direction, and feed parameters are adjusted specifically to ensure that the final path conforms to the motion characteristics of the three-axis machine tool and meets the requirements of ring cutting and equal-distance circumferential processing.

First, perform rough processing: clean the two-dimensional surface. Click on the "2D - Face Milling" option in the top menu bar to open the tool path settings window. Select a 50-millimeter face milling cutter, select the surface area of the workpiece, and process the surface; set the cutting parameters to spindle speed of 5000 revolutions per minute and cutting feed speed of 1000 millimeters per minute, optimize the idle path to reduce non-cutting time. After confirming there are no errors, generate the rough processing tool path.

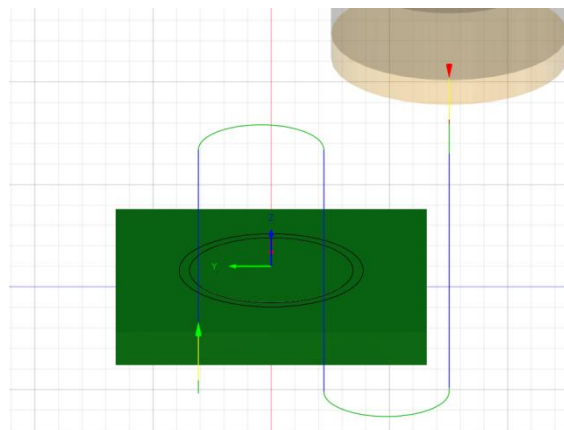


Figure 4.2 Face milling cutter path

Then, use Adaptive Clearing to click on the "3D - Adaptive Clearing" option in the top menu bar to open the tool path settings window. Select a 10mm Flat Endmill and process all the core processing areas of the selected gear chain. This

operation can remove 80% of the excess raw material, making the basic shape of the sprocket clearly visible.

In the outer ring waste removal process, a 2D adaptive cleaning tool is used for efficient rough processing. The specific operation procedure is as follows: Click on the top menu bar of the simulation software, find and select the "2D - Adaptive Cleaning Tool" option. The system will automatically pop up a tool path setting window. In the setting interface, complete the configuration of core parameters such as the selection of the processing area, the definition of the cutting layer, the advance and retreat parameters, and the avoidance distance. Lock the processing target area as the outer ring contour range of the rear sprocket, matching the geometric features of the outer ring and the distribution of the blank waste. Enable the adaptive residual material recognition function.

This process relies on the adaptive cleaning algorithm, which can automatically identify the excess waste in the blank outer ring area, plan the optimal cutting path, and does not require manual setting of cutting parameters layer by layer. It can significantly simplify the programming operation and achieve efficient removal of the blank waste, specifically removing most of the redundant material of the outer ring, quickly forming the basic contour of the outer ring, and leaving uniform remaining space for subsequent ring cutting, circumferential and equidistant precision processing. During the processing, the residual material detection and collision avoidance functions are simultaneously activated, balancing processing efficiency and operational safety, and perfectly adapting to the outer ring rough processing scenarios of the three-axis machine tool.

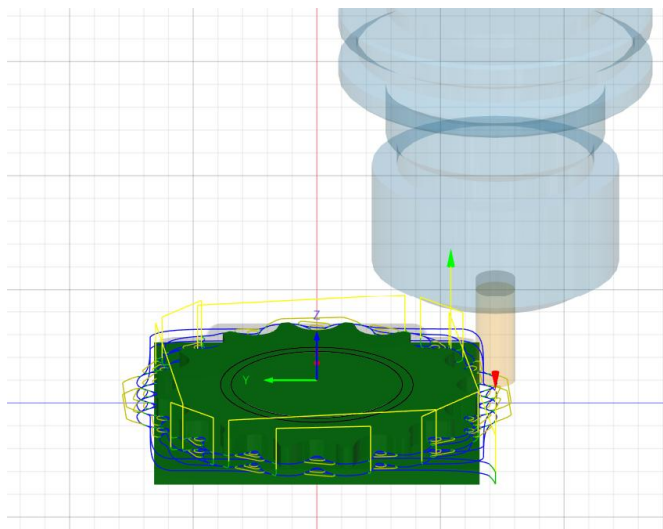


Figure 4.4 2D adaptive path clearing tool path

After completing the adaptive cleaning of the rough machining, the conventional layered cutting process is initiated: during the rough machining stage,

the ring-cutting strategy is adopted throughout the process, with the geometric center of each ring surface as the rotation center, and a constant circular cutting path is set. Further refinement of the outer ring and the rough machining contours of each ring surface is carried out. In the semi-finish machining and finish machining stages, the strategy of circumferential equal-distance cutting is switched. It conforms to the curved surface curvature and contour trend of various ring surfaces, and sets uniform step distances and row spacings. Along the normal direction of the ring surface, equal-spacing layer-by-layer feed is performed, and the corner arc of the tool path, the entry and exit trajectory of the tool, and the elimination of sudden changes in the tool path, hard cuts at the corners, and messy tool marks are refined. After the complete processing path is generated, the path preview function of the simulation platform is activated, and the tool path is checked section by section. Key safety hazards such as broken tools, empty tools, and interference between the tool, the tool holder, and the blank are thoroughly checked. For unreasonable cutting sections, redundant paths, and interference points, the cutting sequence, cutting direction, and feed parameters are adjusted specifically to ensure that the final path conforms to the motion characteristics of the three-axis machine tool and meets the requirements of the entire process.

The teeth have begun to take shape, and the side surfaces of the teeth have been finely milled.

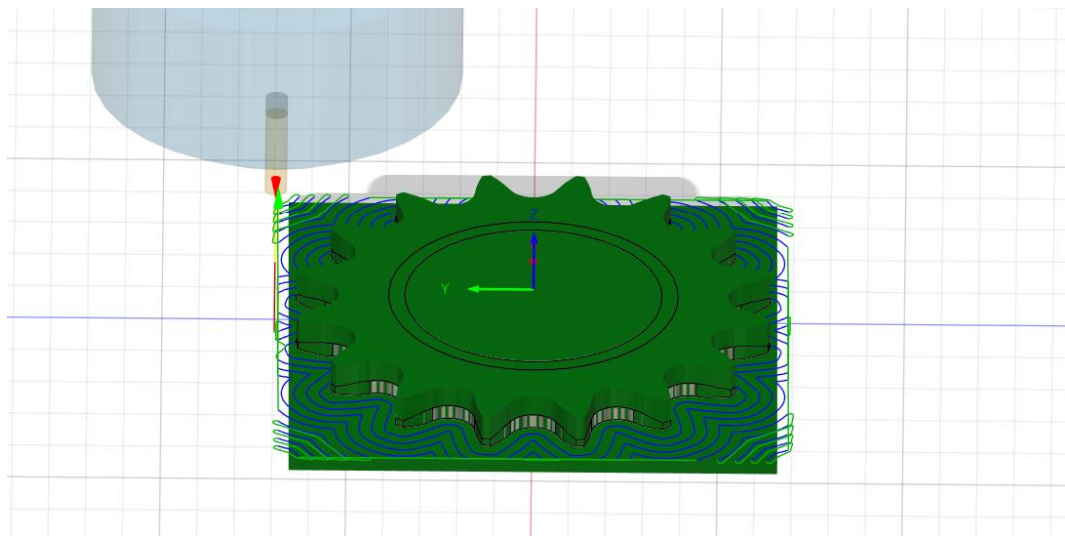


Figure 4.6 Profile milling route for the tooth side surface

After completing the adaptive rough cleaning of the outer ring, the subsequent rough machining process of the transition surface of the rear sprocket is carried out. This process is a crucial link connecting the rough machining of the outer ring and the fine machining of the ring surface. It mainly aims to remove the machining allowance in the arc-shaped transition zone between the inner and outer rings of the rear sprocket and between the end face and the gear ring. Before processing, all the transition surface areas are precisely picked up on the

simulation platform to avoid missed cutting or accidental cutting of adjacent reference surfaces. The overall hard alloy flat-bottomed end mill is still selected for rough machining. By leveraging the axial feed characteristics of the three-axis machine tool, a combined method of layerwise ring cutting and local equal-height cutting is adopted. With the central axis of the transition surface as the rotation reference, the cutting depth is set to decrease layer by layer. Each layer of cutting follows the contour of the surface and makes circular movements, ensuring the rapid formation of the basic contour of the transition surface and avoiding excessive single-cut depth that causes tool overload and workpiece vibration.

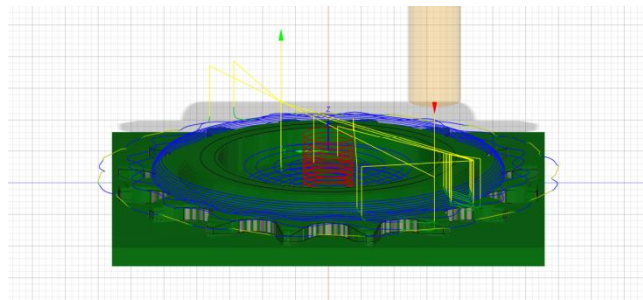


Figure 4.7 Layered incision path

This step not only processes the transitional surface area to prepare for the subsequent use of the Steep Surface and Shallow Plane commands, but also performs a rough processing of the center hole.

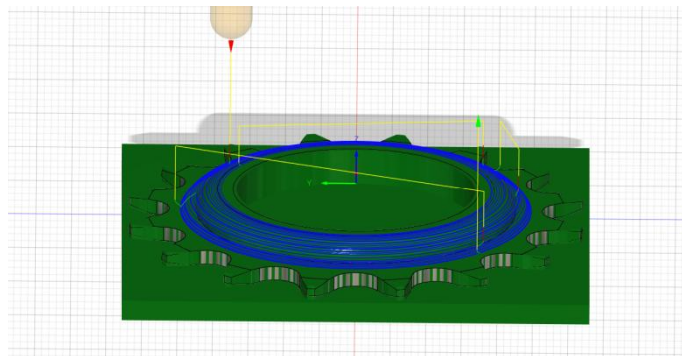


Figure 4.8 Steep surfaces and shallow planes dictate the path

For the tooth root area of this surface, precise and refined processing needs to be carried out simultaneously. This is done to avoid the additional workload caused by secondary clamping and repeated cutting in subsequent processes, and to eliminate the remaining processing allowances, burrs and positional deviations at the tooth root.

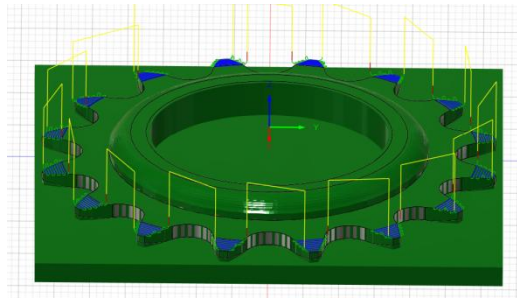


Figure 4.9 Root processing path

For the forming operation of the machined curved surface on the other side of the part, adhering to the principles of process consistency and efficiency, the above-mentioned mature processing approach is adopted to carry out the entire process. Considering the geometric features, precision requirements and structural characteristics of this curved surface, the collaborative processing scheme of pre-processing, transitional surface regularization, key area precision machining and auxiliary hole position rough machining is replicated. The processing is strictly carried out in accordance with the established cutting parameters, path planning and precision control standards, without the need for re-adjusting the tooling, optimizing the processing path or revising the processing instructions. This ensures the uniformity of the machining accuracy, surface quality and form tolerance of both sides of the curved surfaces, and also minimizes the process debugging cycle, avoids the repeated formulation of processing schemes, further improves the standardization degree and production efficiency of the overall processing flow, and ensures the balance and stability of the processing quality on both sides of the part.

The first step is to carry out the rough processing of the surface.

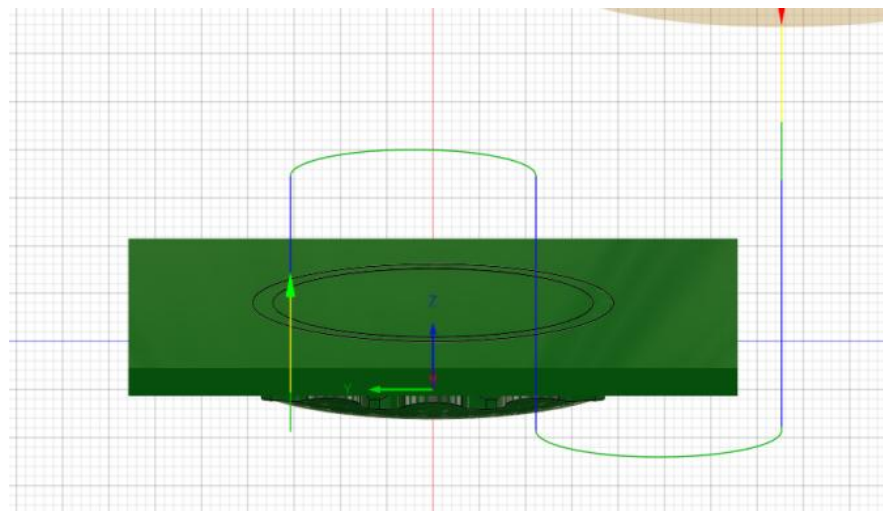


Figure 4.10 Face milling cutter path

Furthermore, for the large amount of leftover raw materials in the processing area of the parts, we adopt two-dimensional adaptive cutting instructions to carry out precise cutting operations. This not only further optimizes the contour shape of the workpiece, but also completely eliminates the excess and redundant parts, clearing the key obstacles for the subsequent processing procedures. During the intermediate stage of part processing, after the initial rough processing and other procedures, the processing area often retains a large amount of irregularly shaped and unevenly distributed leftover materials. If these leftover materials are not handled in time, not only will there be waste of raw materials, but they will also seriously interfere with the precision and efficiency of the subsequent precision processing. Therefore, it is crucial to handle the leftover materials with an efficient and precise cutting method. The two-dimensional adaptive cutting instructions, as an intelligent processing instruction, with its unique adaptive adjustment capability, becomes the optimal choice for handling such leftover materials. It can flexibly adjust the cutting strategy according to the changes in the actual processing scenario, ensuring the targeted and efficient nature of the cutting operation.

With the built-in intelligent path planning function of the two-dimensional adaptive instructions, the system will first precisely scan and identify the two-dimensional contour boundary of the workpiece, and simultaneously collect key data such as the distribution characteristics, thickness differences, and position distribution of the excess materials. Through the built-in algorithm, it conducts rapid analysis and calculation, and automatically generates an efficient and interference-free cutting path. Different from the traditional fixed path cutting method, this intelligent generated cutting path does not require manual intervention and planning by humans. It can fully combine the actual situation of the leftover materials, avoid interference areas such as machine tool fixtures and already processed surfaces, and at the same time minimize the cutting stroke to ensure the smoothness and safety of the cutting process. During the path planning process, the system will prioritize the efficiency of material removal and the regularity of the workpiece contour, optimize the cutting path multiple times to avoid redundant paths and repeated cutting, and improve the overall efficiency of the cutting processing from the source.

During the cutting execution process, the two-dimensional adaptive cutting instructions can precisely locate and remove various leftover materials, including fine residues at the edges and corners of the workpiece, stepwise excess materials generated during processing, and local protruding leftover parts. This ensures that every leftover material can be completely removed, fundamentally avoiding the interference of leftover excess materials on the subsequent precision processing procedures. For example, in subsequent precision processing steps such as grinding and polishing, if there are unremoved residues or protrusions on the workpiece surface, it will cause uneven contact between the processing tool and the workpiece, thereby affecting the processing accuracy and even causing wear and damage to the processing tool. However, through the precise cleaning of the leftover materials by the two-dimensional adaptive cutting, it can provide a flat

and regular processing reference surface for the subsequent processing procedures, ensuring the smooth progress of the subsequent processes.

At the same time, by fully utilizing the flexible characteristics of adaptive cutting, during the cutting process, the cutting speed, feed rate, and other processing parameters can be adjusted in real time according to the thickness, hardness, etc. of the leftover materials. This effectively reduces the idle stroke of the cutting tool and the impact force during cutting, thereby effectively preventing common quality defects such as cracking, deformation, and surface scratches at the workpiece edges. Traditional cutting methods, due to fixed paths and unadjustable parameters, are prone to problems such as excessive cutting force causing workpiece deformation when cutting uneven leftover materials, or insufficient cutting force to completely remove the materials. However, the two-dimensional adaptive cutting instructions, through real-time adaptive adjustment, can always maintain the best state in the cutting process, balancing the thoroughness of material removal and the processing quality of the workpiece, effectively improving the qualification rate of the workpiece.

In addition, this adaptive cutting method can significantly improve the material removal efficiency. Compared with traditional cutting methods, its intelligent path planning and parameter adaptive adjustment functions can significantly shorten the cutting time, reduce ineffective processing steps, and improve the utilization rate of raw materials, thereby reducing production costs. More importantly, through the precise processing of two-dimensional adaptive cutting instructions, the regularity and dimensional accuracy of the overall processing contour of the workpiece can be ensured. This enables the contour error of the workpiece to be controlled within the preset range, laying a stable and reliable processing foundation for subsequent high-precision and precise processing procedures. Ultimately, it ensures the overall quality of the part processing and enhances the competitiveness and practicality of the product.

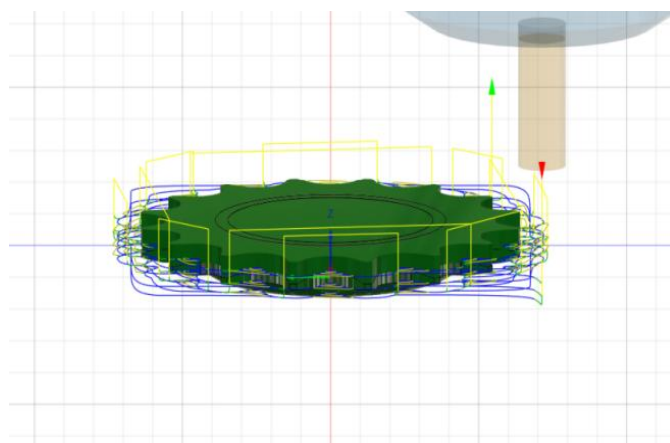


Figure 4.11 2D Adaptive Clearing Path

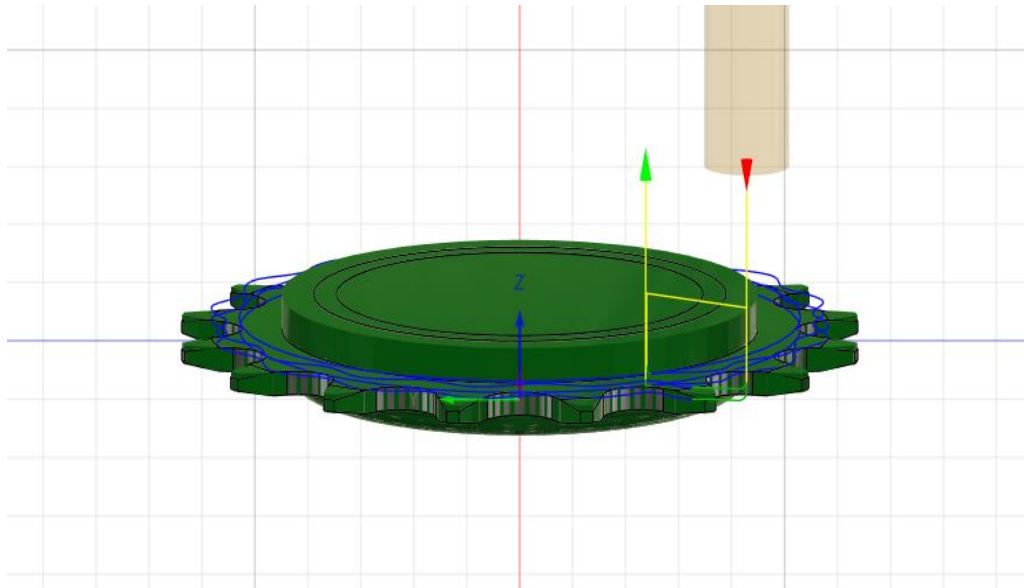


Figure 4.12 2D Adaptive Clearing Path

After completing the adaptive cutting of the remaining raw materials, in order to further enhance the processing regularity and precision consistency of the transition surface area, we adopted a combined processing method of gradient removal and fine removal for this area. Through layer-by-layer and step-by-step refinement operations, we completely removed the residual materials and irregular burrs, ensuring the processing quality of the transition surface. First, we used the gradient removal method to preliminarily regularize the large and widely distributed residual materials in this area. During the processing, we strictly followed the curvature changes of the transition surface and the gradient distribution differences of the remaining materials, and carried out cutting operations in a hierarchical and controlled manner to effectively avoid surface deformation and tool vibration caused by excessive load during a single cut. At the same time, this reserved uniform and regular processing allowance for the subsequent fine processing. Subsequently, we carried out targeted fine removal operations, focusing on the edges, corners, and transition connection areas of the transition surface, to precisely shape and refine, precisely eliminating local irregularities and contour deviations caused by the remaining materials, further optimizing the smoothness of the transition surface, ensuring the dimensional consistency of each boundary area, and maximizing the execution requirements of subsequent processing instructions, laying a solid foundation for the precision control of the entire fine processing process.

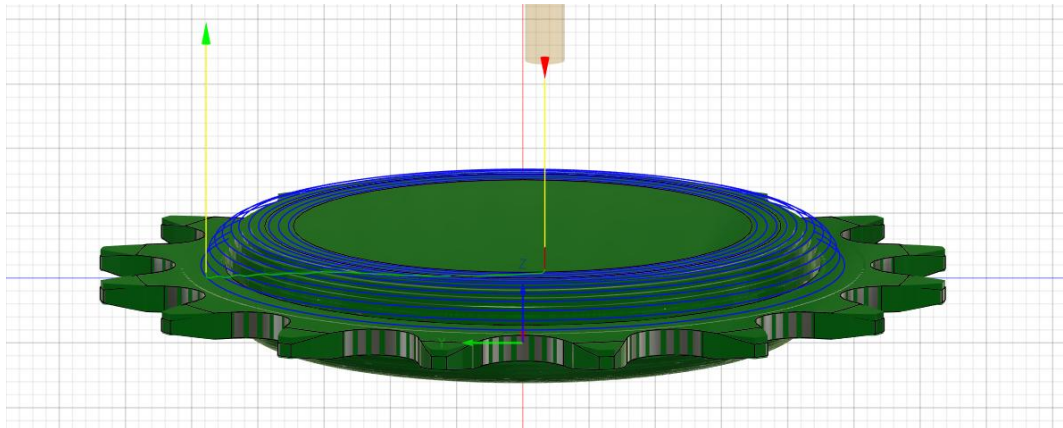


Figure 4.13 Gradient clearing

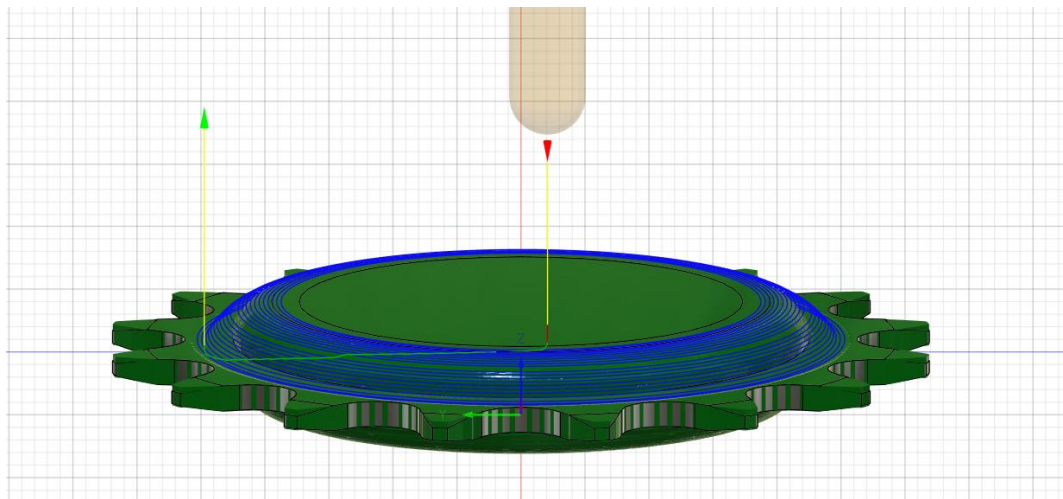


Figure 4.14 Precise cleaning

The surface-root area needs to undergo both precise and meticulous processing to achieve the final shape. This area is crucial for the connection of the workpiece, and the processing quality directly determines the overall accuracy, structural stability, and usage reliability. Any deviations or roughness can lead to stress concentration, assembly difficulties and other potential problems. Precise processing requires strict control of tolerances, using high-precision equipment to monitor and calibrate parameters to avoid edge breakage and missing corners; meticulous processing needs to ensure a smooth surface, remove burrs and scratches, and ensure a round connection. The combination of the two, following the process specifications, can complete the shaping and ensure that the workpiece meets the standards.

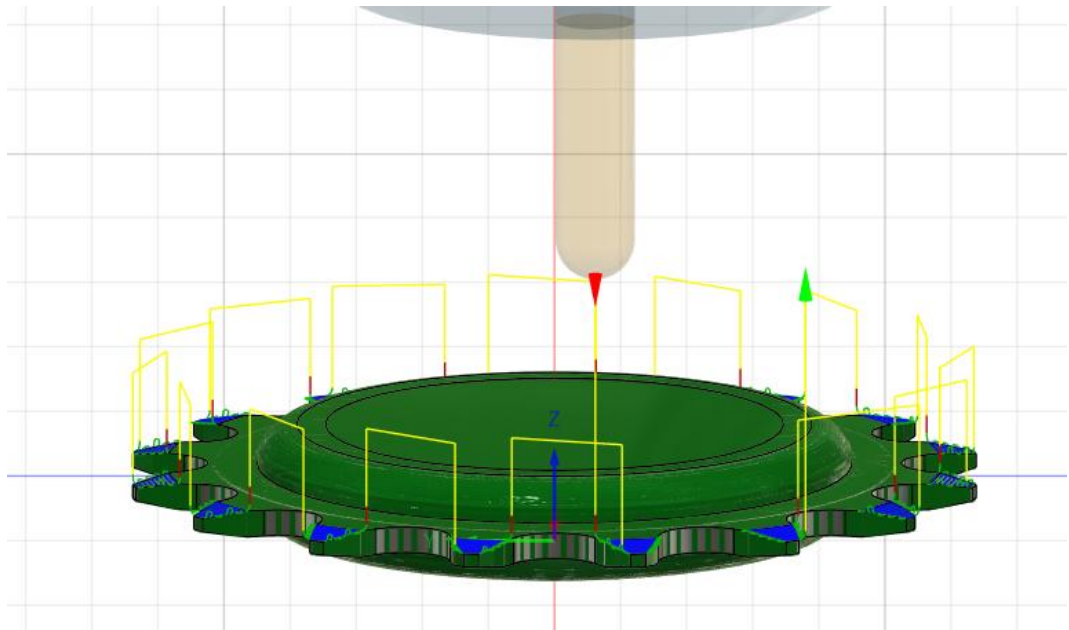


Figure 4.16 Root area path

After the fine processing of the transition surface area is completed, the final step of the simulation process is to focus on handling the center hole issue. The center hole serves as the core reference basis for subsequent workpiece positioning, assembly, and further precision processing. The quality of its processing directly determines the final accuracy and reliability of the entire simulation process, and is crucial for the success or failure of the subsequent actual processing. Therefore, strict and meticulous quality control must be carried out. During the processing of the center hole, we follow a standardized process and gradually advance: Firstly, we use a combination of high-pressure air blowing and special cleaning tools to thoroughly remove the residual iron filings, cutting fluid residues, and other impurities in the center hole, to avoid these foreign substances causing gap deviations during subsequent positioning, and ensure the cleanliness of the positioning reference. Subsequently, we use high-precision special calibration tools to precisely calibrate the coaxiality and verticality of the center hole, strictly controlling the size deviation within the preset tolerance range, ensuring a seamless and precise fit between the center hole and the reference surface of the workpiece, and providing a guarantee for the positioning accuracy of the subsequent processing. At the same time, with the help of magnifying glasses and other auxiliary tools, we carefully inspect the smoothness of the inner surface of the center hole, and finely polish off the burrs and scratches at the hole opening and inner wall to prevent surface defects caused by subsequent processing from leading to positioning deviation, uneven force, and subsequent deformation or processing errors of the workpiece. Only by completing the entire process of center hole processing in a standardized and refined manner can the entire processing simulation process form a complete closed loop, providing a

scientific and reliable reference basis for the subsequent actual processing, and ensuring the accuracy and efficiency of actual production.

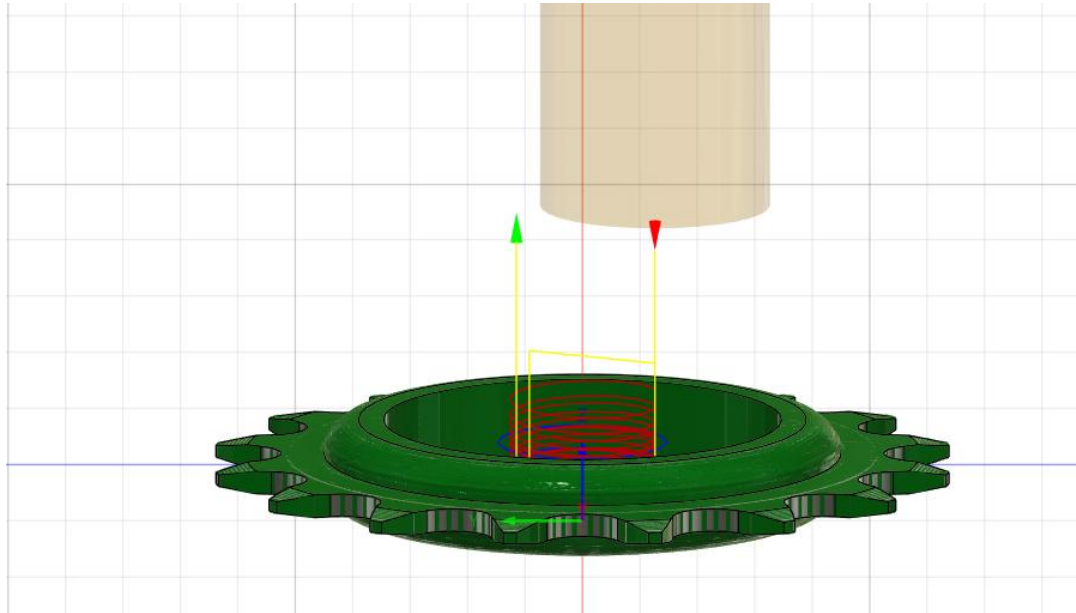


Figure 4.17 Center hole processing path

At the initial stage of the precision manufacturing process, we use the Fusion 360 software, leveraging its path generation function to precisely plan the cutting paths based on the design drawings and process requirements, ensuring that the operation aligns with the design intent. After the planning is completed, we will use the built-in analysis tools in the software to conduct a detailed verification of the cutting paths, checking for continuity, smoothness, and whether they meet the process standards, such as cutting depth, speed, angle, etc.

Once the verification is satisfactory, we use the advanced simulation commands of the machine tool to simulate the real cutting environment, including material properties, tool wear, machine dynamics, and other factors. We conduct a comprehensive inspection of the cutting process from all aspects. During the process, we identify and record all error or warning messages, and promptly adjust and optimize.

After rigorous verification, the simulation steps are accurate and error-free. The cutting path planning has been verified both in theory and in the simulation environment, ensuring that the actual production is of high quality and efficiency. Based on this, we can advance to the production simulation stage, simulating the entire production process to ensure the smooth progress of precision manufacturing.

5 FEM Analysis for the chain transmission

5.1 Finite Element Theory Foundation

ANSYS is a software used for finite element calculations. Since the first ANSYS software was introduced in 1970, it has undergone more than 40 years of development and has gradually become a leader in the field of finite element analysis. This software can interface with a variety of mainstream CAD software. In the past few decades, the development of the finite element method has been rapid. It is widely used in the nuclear industry, railways, petrochemicals, aerospace, etc. Currently, more and more universities offer courses on finite element analysis, and many schools use ANSYS software for finite element analysis. It has been widely accepted internationally.

ANSYS has some functions of physical models, but compared with other modeling software, its functions are not very powerful. It can store models that have been completed in other software into ANSYS and then proceed with the next operation. The introduced model should be simply processed first. After the processed entities are segmented for meshing, material properties are imported, loads and constraints are input, etc., the solution results can be obtained to determine whether the structural strength of the transmission system meets the requirements. This is not only a key concern for mechanical designers but also for product users. The structural strength of the transmission system must not only meet the usage requirements but also retain safety margins. As the transmission system is an important structure of bicycles, it is affected by various complex road conditions during use, which is of great significance for ensuring the safety of use.

Finite element method (FEM) is a method used in structural mechanics for discrete structure analysis. The core idea of the finite element method can also be summarized as "divide the whole into parts" and "divide the parts into the whole". This section uses the finite element software Ansys to conduct stiffness analysis of the supporting structure, explore the stress distribution and deformation characteristics of the transmission system under given conditions, and provide data basis and theoretical support for the final design.

5.2 Geometric modeling and material property setting

The three-dimensional model structure used in this finite element analysis is relatively simple. The overall shape is simple and regular, without complex irregular structures. It is mainly composed of basic geometric shapes. During the model construction process, in order to match the actual processing conditions and reduce the phenomenon of structural stress concentration, rounded corner features were added to the edges and connection parts of the model. This feature not only

conforms to the processing logic in actual production but also can more realistically reflect the stress state of the structure. It should be particularly noted that if all these geometric features such as rounded corners are removed, it will cause deviations in the geometric shape of the model from the actual structure, thereby affecting the rationality of meshing in the finite element analysis process and the accuracy of stress calculation. It may lead to distorted calculation results in the stress concentration areas and fail to truly reflect the actual stress condition of the structure. Therefore, considering the reliability and accuracy of the analysis results, it was ultimately decided not to clear the geometric features of this structure. The specific three-dimensional model used in this finite element analysis is shown in Figure 5.1. This model retains all the geometric features added during the modeling process, providing a reliable model foundation for the subsequent analysis work.



Figure 5.1 Import the three-dimensional model into ANSYS.

5.2.1 Ansys Analysis

Since the load on the sprocket is a stable load in the constant-speed driving state, the rotational speed is relatively low and the inertia effect can be ignored. Therefore, a static structural finite element analysis is adopted for the chain drive and sprocket structure to calculate the stress distribution and deformation, and to verify its strength and stiffness. The static mechanical module in Ansys Workbench is used to conduct a static strength analysis of the transmission structure. Subsequently, the model is verified to meet the stiffness requirements for actual use, and then modal analysis can be conducted. The modal analysis and static mechanical analysis modules are shown in Figure 5.2

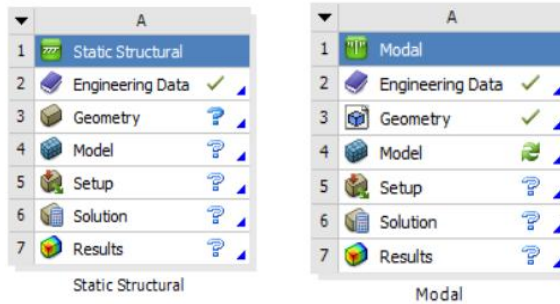


Figure 5.2 Ansys Static Structural Module and Modal Module

5.2.2 Material Assignment

The transmission structure, as the core component of a mechanical device, usually needs to have high strength while also maintaining light weight. Its materials are typically obtained through processes such as metal heat treatment. Therefore, the sprocket is made of aluminum alloy, and the roller chain is made of structural steel. According to the query of relevant literature, the elastic modulus of aluminum alloy is 71.7 GPa, the Poisson's ratio is 0.33, the density is 2.81 g/cm³, and its yield limit is 280 MPa. In the finite element analysis, the parameters of aluminum alloy are shown in Figure 5.3, and the material properties of each component are detailed in Table 4.

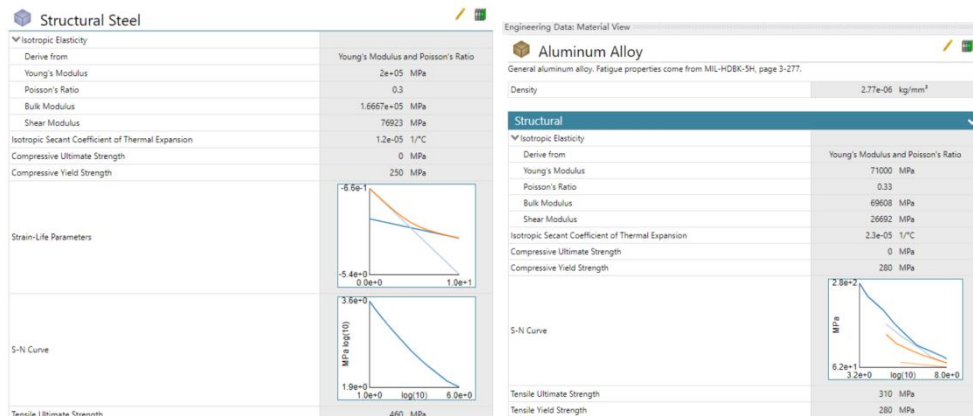


Figure 5.3 Material Library

Table 4. Material properties of each component

Component	Materials	Density (g/cm ³)	Elastic modulus (GPa)	Poisson's ratio (μ)
Sprocket	Aluminum alloy	2.81 g/cm ³	71.7 GPa	0.33
Sprocket chain	Structural steel	7.85 g/cm ³	210 GPa	0.3

5.2.3 Model Import

Considering that the three-dimensional drawing function provided by the finite element analysis software is not only complex in operation but also has obvious limitations in geometric feature drawing and detail processing, making it difficult to efficiently draw a three-dimensional model that meets the analysis requirements and has detailed features, we have chosen the Solidworks software for the drawing of the three-dimensional model in this analysis. The Solidworks software has the advantages of convenient operation and comprehensive functions, which can accurately present the basic geometric structure of the model and add key features such as chamfers. This fully meets the requirements of the analysis for model accuracy. After the model is drawn, we will import the three-dimensional model generated by the Solidworks software into the Ansys Workbench finite element analysis software. After the import, through the "Discovery" page in the software, a comprehensive check of the imported three-dimensional model is conducted. The core purpose of this check is to verify whether there are problems such as geometric feature loss, shape deformation, or detail damage during the import process, ensuring that the imported model is completely consistent with the original drawn model, and providing a precise and reliable model support for subsequent meshing, stress calculation, and other finite element analysis steps. The specific three-dimensional model imported into the finite element software in this analysis is shown in Figure 5.4.



Figure 5.4 The three-dimensional models in Discovery

5.3 Grid Division and Boundary Conditions

5.3.1 Grid division

Based on the operating characteristics of the bicycle, the operation status of the transmission structure is mostly in a state of vibration and shaking, and there are many rotatable rods. Therefore, the meshing of the transmission structure adopts the dominant entity element of the main quadrilateral, and the mesh size is set to the default. The finite element model of the transmission mechanism is shown in the figure, consisting of 28571 elements and 67356 nodes.



Figure 5.5 Model grid division

5.3.2 Boundary condition setting

First, set up two sprockets and align the centers of the two sprockets to form a rotational pair for the object relative to the ground.

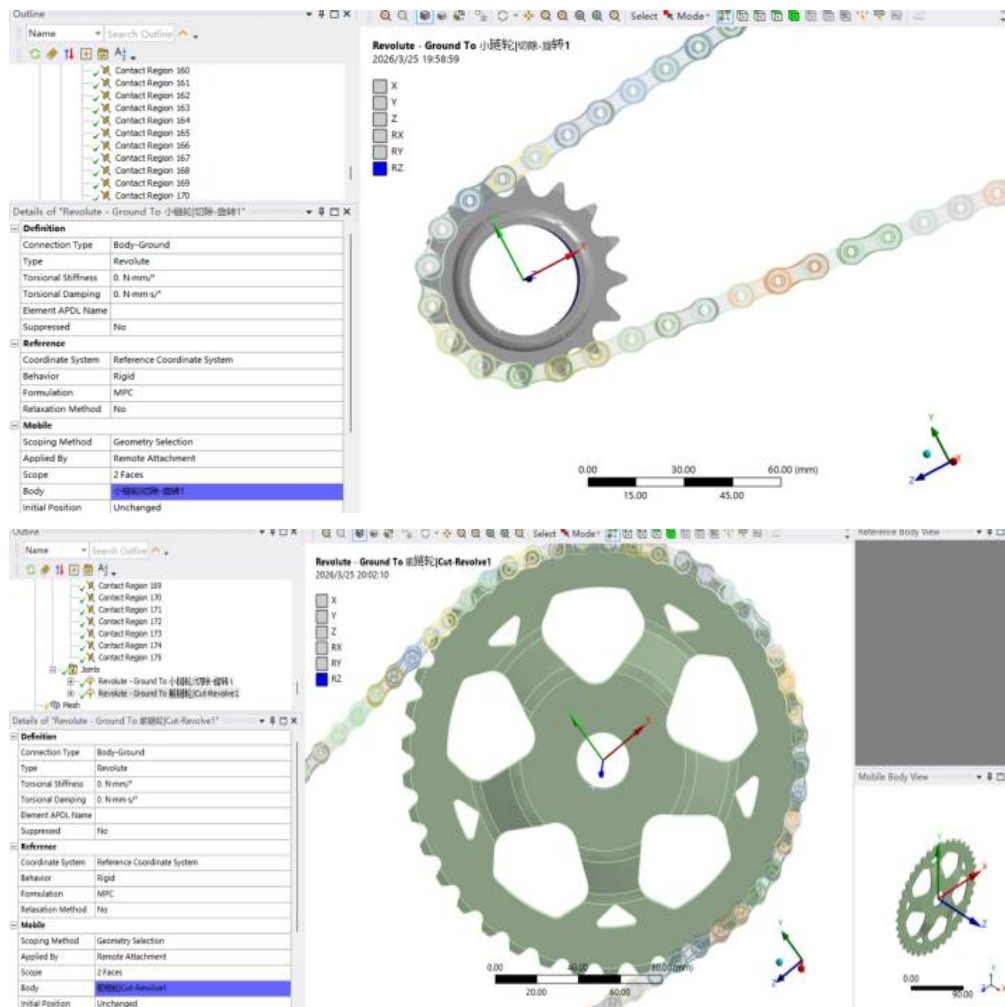


Figure 5.6 Rotary joint setup

A cylindrical support piece was specially set at the center position of the drive sprocket. This support piece precisely fits the center hole of the drive sprocket and plays a crucial role in fixing and supporting the sprocket. To simulate the actual working condition of the drive sprocket and ensure that the constraints of the finite element analysis are in line with the actual situation, this cylindrical support piece is subjected to fixed constraints in both the axial and radial directions, achieving complete locking. This effectively restricts the axial movement and radial deviation of the sprocket, avoiding deviations in the analysis results due to improper constraints. At the same time, in accordance with the working requirements of the drive sprocket, this support piece retains the tangential degree of freedom, allowing the sprocket to rotate smoothly around the support piece. This truly recreates the working scene of the sprocket transmitting power and driving the chain movement in actual operation, providing realistic constraints for

subsequent analysis of key parameters such as the force distribution and torque transmission of the sprocket.

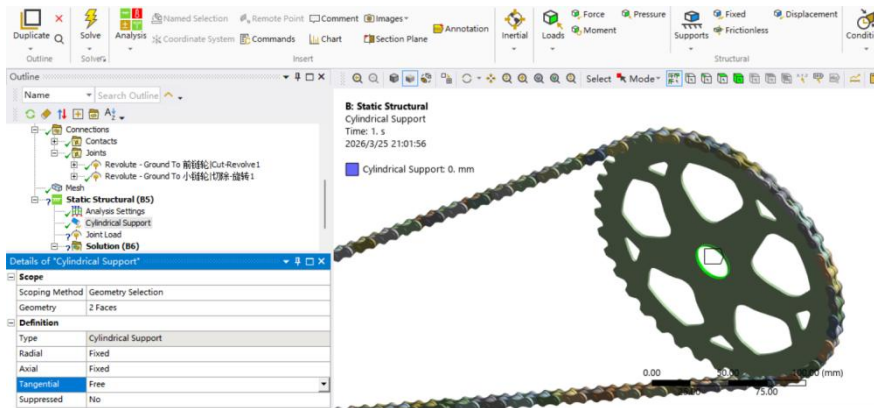


Figure 5.7 Cylindrical support

The torque acting on the transmission structure is mainly generated by the driving wheel. Therefore, we perform the calculation based on the given conditions. The general formula for the torque of rotation is $T = 9550 \cdot \frac{P}{n_1}$ (where P represents power in kilowatts, n_1 represents rotational speed in revolutions per minute, and T is in (N·m)

$$T = 9550 \cdot \frac{P}{n_1} = 9550 \cdot \frac{1.617}{40} \approx 386 \text{ N}\cdot\text{m} \quad (14)$$

Based on the calculation results, an additional rotational load is applied to the driving pulley, and the type of this load is torque.

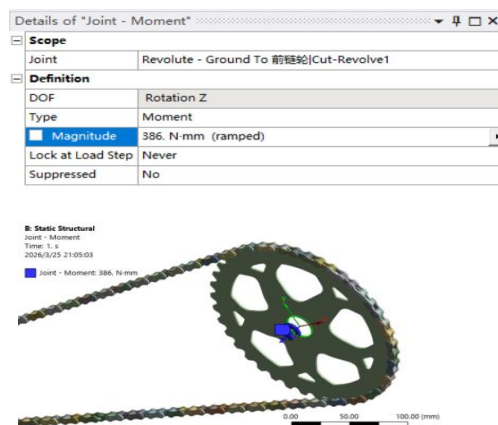


Figure 5.8 joint load setup

5.4 FEM analysis

5.4.1 Static analysis

After determining the above typical working states, the preset solution conditions were set, and numerical simulations were conducted on them. The following conclusions were drawn. The strength of the transmission structure refers to the ability of the transmission structure to withstand compression and tension. The equivalent stress diagram under normal conditions was obtained through ANSYS, and it was found that the maximum yield strength of the structure under this state was 3.5177 MPa, and the maximum deformation was only 0.0337 mm, which met the strength requirements.

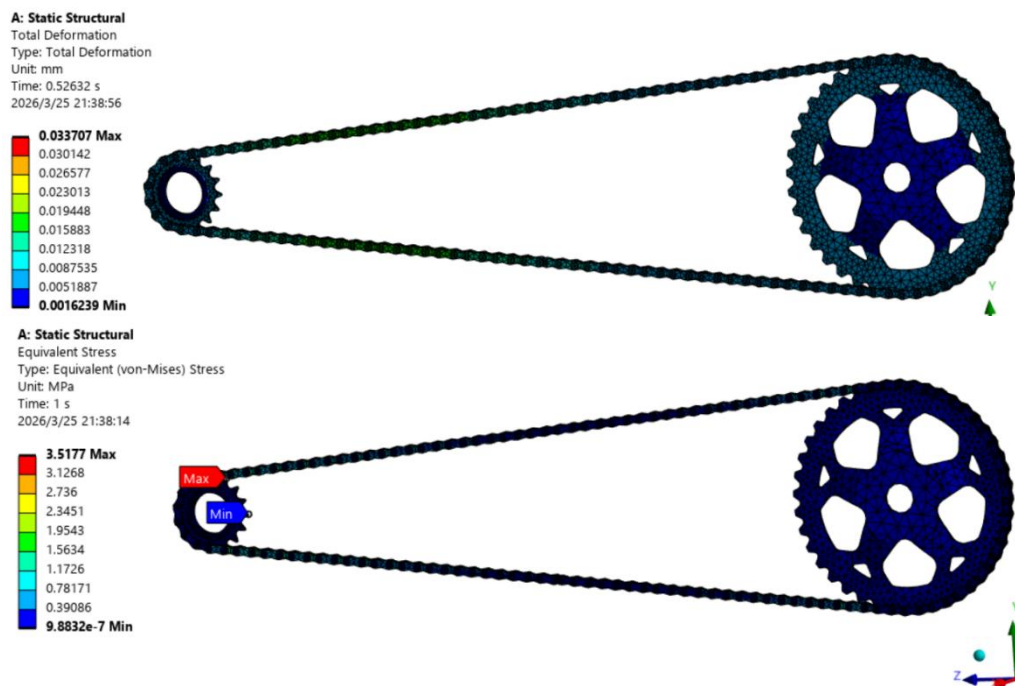


Figure 5.9 Deformed cloud map and stress cloud map

5.4.2 Modal analysis

Modal analysis theory is derived by integrating analysis from vibration theory, structural mechanics, calculus and other dynamic and mathematical theories. It is a reliable indicator for measuring the dynamic performance of mechanical structures, and is a crucial theoretical basis for fault diagnosis, fault investigation and optimization design of mechanical structures, with significant reference value.

The modal method is a means for studying the dynamic performance of structures. It has been widely applied in actual engineering. Based on this, a new calculation method was proposed and this method was improved. From the

perspective of mechanics, a multi-degree-of-freedom linear equation system was constructed using the finite element method:

$$mx + cx + \ddot{k}x = f(t) \quad (15)$$

Here, m represents the mass matrix, c represents the damping matrix of the system, and k represents the stiffness matrix of the system. x and f represent the displacement and excitation force of the system.

Based on this, the relationship between the dynamic response and the dynamic response itself was analyzed, and a dynamic response analysis method based on the dynamic response was proposed. Therefore, in this case, the damping has a very small effect on the system.

$$mx + \ddot{k}x = 0 \quad (16)$$

A fixed mode analysis was conducted on the two sprocket wheels, still using the cylindrical fixed support as before. The frequencies of the first six non-rigid modes were calculated, and the first six vibration modes were obtained. The following results are shown in the figure.

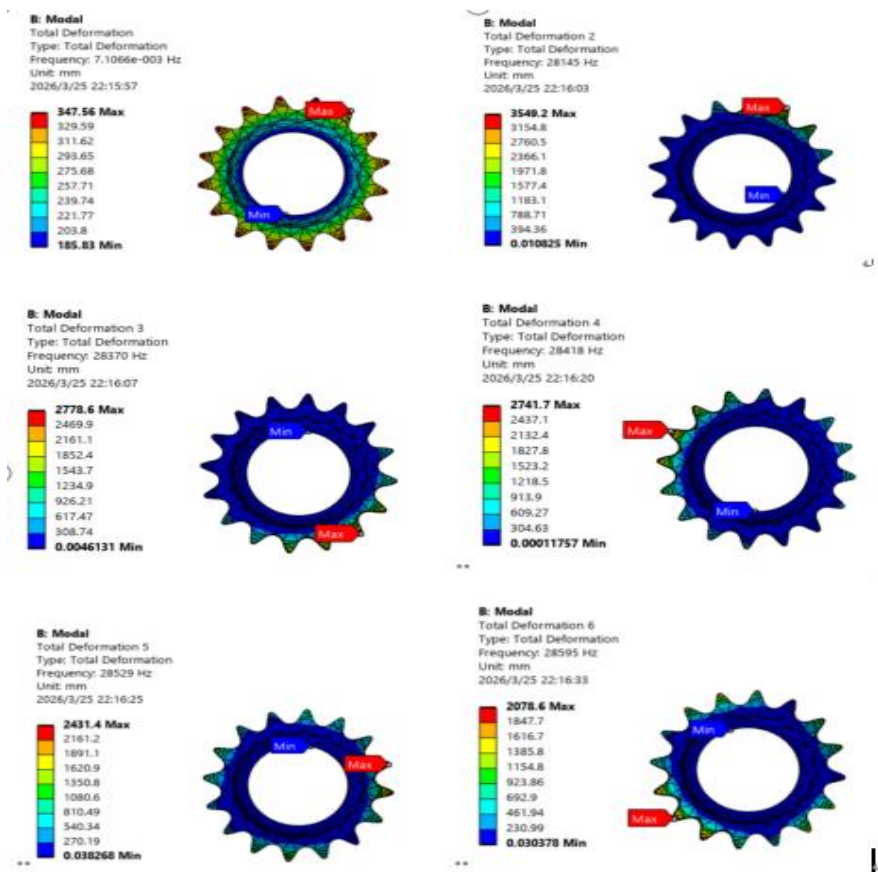


Figure 5.10 The sixth-order non-rigid mode frequency before the back sprocket

The summary of the natural frequencies and vibration modes of the back sprocket is shown in the table 5.

Table 5. Natural frequency and its mode of vibration

Mode	Frequency (Hz)
1	7.1066e-003
2	28145
3	28370
4	28418
5	28529
6	28595

The sixth-order vibration mode of the front sprocket is shown in the figure.

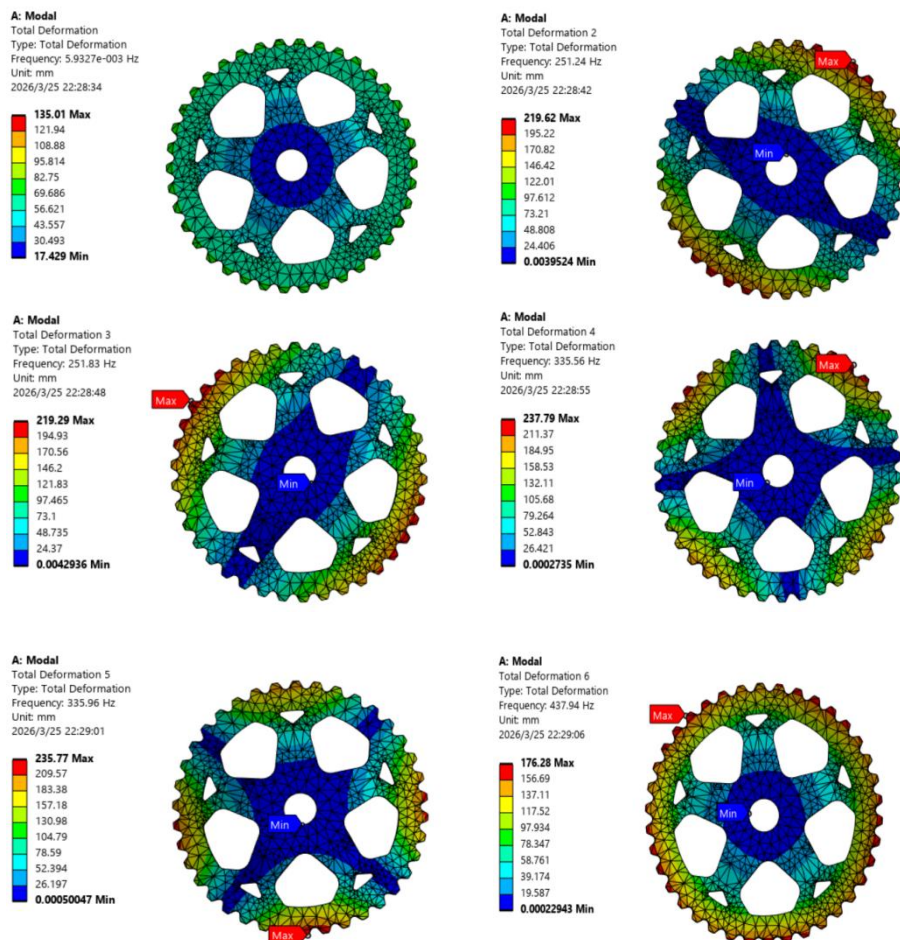


Figure 5.11 The sixth-order non-rigid mode frequency before the front sprocket

The summary of the natural frequencies and vibration modes of the front sprocket is shown in the table 6.

Table 6 Natural frequency and its mode of vibration

Mode	Frequency (Hz)
1	5.9327e-003
2	251.24
3	251.83
4	335.56
5	335.96
6	437.94

Based on the results of the modal simulation, it is evident that in the first six modes, the vibration frequencies of both sprockets are relatively high. This indicates that the sprockets belong to a high-frequency system and possess relatively strong high-frequency characteristics. The main content of this chapter is to conduct simulation and analysis of the static mechanics and modal of the transmission structure, as well as to verify its static mechanical performance. It also simulates the operating conditions and verifies that the stress and deformation meet the material and strength requirements, and the structure is relatively stable. Since bicycles generate vibrations during operation, the modal analysis of the sprocket is carried out to meet the requirements of dynamic performance. Through the analysis of the first six modes, it is concluded that the structure can maintain a stable structure under operating conditions and the safety performance is guaranteed.

6 Conclusion

This research conducted a comprehensive and systematic study on the design optimization and performance verification of the bicycle chain drive system. The core research objective was to solve the core contradiction of traditional bicycle drive systems, which is the difficulty in balancing lightweight, structural reliability, and processing economy. The research aimed to provide a technical solution with both theoretical value and engineering application value for the upgrade and iteration of the bicycle drive system. At the beginning of the research, through literature review and industry research, the current research status, technical development trends, and existing bottlenecks of bicycle drive mechanisms at home and abroad were systematically summarized. The technical characteristics, application scenarios, and advantages and disadvantages of different drive schemes were analyzed in detail, including chain drive, synchronous belt drive, and shaft drive, the three mainstream drive forms. Through quantitative comparison and qualitative analysis of key indicators such as transmission efficiency, load-bearing capacity, lightweight potential, maintenance cost, processing difficulty, and adaptability of the three drive schemes, a mature, high-efficiency, widely adaptable, and cost-controllable roller chain drive system was finally determined as the core research object of this study. Based on the actual riding conditions of bicycles, the parameters of core components such as sprockets and chains were parameterized for design, and the key dimensions, material selection, and structural parameters of each component were clarified, laying a solid foundation for subsequent modeling and simulation work.

Based on the determined design scheme, this research completed the full parameterization modeling of the bicycle chain drive system using professional three-dimensional modeling software (such as SolidWorks). During the modeling process, the design parameters of each component were strictly followed to ensure the accuracy and correlation of the model, enabling adjustable and optimized key parameters such as the number of teeth of the chain wheel, tooth shape parameters, chain pitch, etc. This provided convenience for subsequent design iterations. After completing the full parameterization modeling, the transmission system was subjected to systematic static and dynamic simulation analyses using finite element analysis software (such as ANSYS) to fully verify the rationality and reliability of the design scheme. The static simulation analysis mainly simulated the static load borne by the transmission system under normal bicycle riding conditions (rated load, regular riding speed), focusing on analyzing the stress distribution, deformation, and load-bearing capacity of the transmission structure. The static analysis results showed that under the rated load of normal bicycle riding, the maximum equivalent stress of the transmission structure was only 3.5177 megapascals, and the maximum deformation was only 0.0337 millimeters; compared and verified, this maximum equivalent stress was far below the yield strength of the selected material, and the maximum deformation was also within a

very small range. This result fully confirmed that the design scheme had excellent strength reliability under static load conditions, and also verified that the structure design retained sufficient load-bearing capacity while achieving the lightweight goal, meeting the static load-bearing requirements of bicycles under different riding conditions, effectively solving the problem of mutual constraint between lightweight and load-bearing capacity in traditional designs.

To further comprehensively evaluate the dynamic performance of the transmission system and avoid structural failure risks during dynamic operation, this study conducted modal analysis on the transmission system, extracting the first to sixth natural frequencies and corresponding vibration modes of the front and rear chain wheels. Through the analysis of natural frequencies and vibration characteristics, the dynamic response laws of the transmission system were clarified. The modal analysis results showed that the low-order natural frequencies of the front and rear chain wheels were at extremely low levels, far below the working frequency range of bicycles during normal riding, while the high-order natural frequencies reached 250 hertz to 430 hertz and above. Combined with the working frequency range of the transmission system of the bicycle during normal riding (usually within tens of hertz), it could be determined that this drive system belongs to a typical high-frequency system. This key characteristic implies that within the full operational range of bicycle riding, the working frequency of the transmission structure does not overlap with its own natural frequency, effectively avoiding the occurrence of resonance. This ensures the structural stability and operational safety of the transmission system during dynamic operation, significantly reducing early failure issues such as increased wear on chainwheel tooth surfaces, chain fatigue fractures, and loosening of connecting components caused by resonance. It also extends the service life of the transmission system and enhances the reliability and comfort of bicycle riding.

In terms of processing technology and process optimization, this research fully integrates actual industrial production conditions, taking into account both processing accuracy and economic requirements. It selects a three-axis vertical machining center as the core processing equipment for chainwheel and other core components. Compared to a five-axis machining center, this approach effectively reduces equipment investment costs and production operation costs. At the same time, through process optimization, the shortcomings of the three-axis processing equipment in complex surface processing are compensated. Based on the selected processing equipment, a scientific and reasonable double-sided processing route was formulated, clarifying key process links such as processing procedures, tool selection, cutting parameters, and positioning methods. Specifically, the processing path and process connection were optimized according to core processing requirements such as chainwheel tooth shape accuracy, hole position coaxiality, and end face flatness. Through simulation and actual debugging verification of the processing path, this process scheme effectively avoids risks such as overcutting and tool collisions during the processing process, ensuring that key indicators such as tooth profile accuracy and tooth pitch error of the chainwheel meet design requirements. At the same time, it significantly improves

the standardization of the processing program, shortens the process debugging cycle, and reduces the skill requirements for operators. It provides a feasible technical reference and process support for the large-scale batch production of such transmission components, achieving an organic balance between processing quality and economic efficiency.

In summary, through a series of systematic works including theoretical analysis, parametric design, three-dimensional modeling, simulation verification, and process optimization, this research completed the design optimization and performance verification of the bicycle chain transmission system. The rationality, feasibility, and superiority of the design scheme have been fully demonstrated through theoretical analysis and simulation verification. This design scheme not only fully meets the core performance requirements of the bicycle transmission system in terms of strength, stiffness, and dynamic stability, effectively addressing the pain points of traditional transmission systems in balancing lightweight, reliability, and processing economy, but also fully considers the actual needs of industrial production, balancing processing costs and production efficiency. It provides a solid theoretical basis, technical support, and practical reference for the lightweight design, performance improvement, and industrial application of the bicycle transmission system, and has significant practical significance and application value for promoting the technological upgrading of the bicycle transmission system and improving the overall quality of bicycle products. Further research can be conducted based on this, combined with actual riding tests to further verify the practical application effect of the design scheme, and can also conduct further optimization design for extreme riding conditions (such as heavy-load climbing, long-term high-speed riding) to further improve the comprehensive performance of the transmission system.

List of references

- [1] “- The Curious Case of Leonardo da Vinci’s Bicycle,” CapoVelo.com, Aug. 19, 2020. <https://capovelo.com/curious-case-leonardo-da-vincis-bicycle/>
- [2] “Rover ‘Safety’ Bicycle, 1885,” Sciencemuseumgroup.org.uk, 2024. <https://collection.sciencemuseumgroup.org.uk/objects/co25833/rover-safety-bicycle-1885>
- [3] David Rome, “Pro bike: José Antonio Hermida’s Merida Big.Nine,” Jun. 31, 2014. <https://www.bikeradar.com/features/pro-bike/pro-bike-jose-antonio-hermidas-merida-big-nine>
- [4] SODEN P D, ADEYEFA B A. Forces applied to a bicycle during normal cycling[J]. Biomech, 1979, 14:843-856.
- [5] RAY P S H, THOMLINSON Ma, TU Y S. Kinematics and kinetics of a non-circular bicycle drive system[J]. Mechanism and Machine Theory, 1991, 44:383.
- [6] Getz NH, Marsden JE. Control for an autonomous bicycle//Proceedings of 1995 IEEE International Conference on Robotics and Automation. IEEE, 1995, 2:1397-1402
- [7] Boyer F, Perez M, Mauny J. Reduced dynamics of the nonholonomic Whipple bicycle. Journal of Nonlinear Science, 2018, 28(3):943-983
- [8] Basu-Mandal P, Chatterjee A, Papadopoulos JM. Hands-free circular motions of a benchmark bicycle. Proceedings of the Royal Society A: Mathematical, Physical and Engineering Sciences, 2007, 463(2084):1983-2003
- [9] 张健, 李昕. “对自行车运动员在骑行过程中踏蹬动作的生物力学分析.” 北京体育师范学院学报 .01(1997):52-55. doi:10.14036/j.cnki.cn11-4513.1997.01.010 ??.
- [10] Wu Shangsheng. Analysis of Bicycling State Based on Linkage Model of Human-Bicycle[J]. Journal of South China University of Technology (Natural Science Edition), 2016, 44(2): 46-52,59.
- [11] Cong, Chen and Vr Lab. “An Investigation of Bicycle Dynamics in Interactive Bicycle Simulator.” (2004).
- [12] TheFuture, “Autovelo Electric Bike Is An Ultimate Short Distance Urban Transportation Alternative - Tuvie Design,” Tuvie Design, Apr. 15, 2010. <https://www.tuvie.com/autovelo-electric-bike-is-an-ultimate-short-distance-urban-transportation-alternative/> (accessed Dec. 05, 2025).
- [13] TheFuture, “Collapsible Bicycle Concept by Blair Hasty - Tuvie Design,” Tuvie Design, Aug. 21, 2008. <https://www.tuvie.com/collapsible-bicycle-concept-by-blair-hasty/> (accessed Dec. 05, 2025).
- [14] “基于情感需求的太空自行车造型设计研究,” Zhangqiaokeyan.com, 2019. https://www.zhangqiaokeyan.com/academic-degree-domestic_mphd_thesis/020315227159.html (accessed Dec. 01, 2025).
- [15] “可变形儿童自行车创新设计研究,” Zhangqiaokeyan.com, 2018. https://www.zhangqiaokeyan.com/academic-degree-domestic_mphd_thesis/020315049724.html (accessed Dec. 01, 2025).
- [16] R. McAllister, “Parts Of A Bicycle Explained: Comprehensive Guide To Your Bike,” BikeTips, Jan. 02, 2024. <https://biketips.com/parts-of-a-bicycle-explained/>
- [17] Lovejoy, K.; Handy, S. Developments in bicycle equipment and its role in promoting cycling as a travel mode. In City Cycling; MIT Press: Cambridge, MA, USA, 2012; pp. 75-104.
- [18] Stead Cycles. Single Speed vs Geared Bikes. 2023. Available online: <https://www.steadcycles.com.au/singlespeed-vgearedbikes/> (accessed on 23 March 2023).
- [19] Urunkar, R.U.; Deshpande, P.P. Study of Drive Mechanisms of Bicycle, Tricycle or Like Vehicles to Optimize Operating Performance-A Review. J. Eng. Res. Appl. 2014, 4, 214-219. Available online:

[https://www.ijera.com/papers/Vol4 ISSUE1/Version%202/AC4102214219.pdf](https://www.ijera.com/papers/Vol4%20ISSUE1/Version%202/AC4102214219.pdf) (accessed on 28 October 2024).

[20] Stratview Research. Belts, Chains and Gears: How Power Transmission Works. EETech Media. 2022. Available online: <https://eepower.com/technical-articles/belts-chains-and-gears-how-power-transmission-works/#> (accessed on 24 March 2023).

[21] SRAM. Spare Parts Catalog; SRAM: Chicago, IL, USA, 2023. [CrossRef]

[22] Reiter, M.; Florczyk, R.; Braedt, H. Chainring. U.S. Patent US 11,110,991 B2, 7 September 2021. Available online: <https://patents.justia.com/patent/11110991> (accessed on 10 January 2025).

[23] Cho, C.K.; Yun, M.H.; Yoon, C.S.; Lee, M.W. An ergonomic study on the optimal gear ratio for a multi-speed bicycle. *Int. J. Ind. Ergon.* 1999, 23, 95-100. <https://www.sciencedirect.com/science/article/abs/pii/S0169814197001042?via%3Dihub>

[24] van Soest A. J. (2014). From bicycle chain ring shape to gear ratio: algorithm and examples. *Journal of biomechanics*, 47(1), 281–283. <https://doi.org/10.1016/j.jbiomech.2013.10.025>

[25] Mo, Y.; Xu, X. Solidworks chain drive design and 3D modeling techniques. *Appl. Mech. Mater.* 2012, 215-216, 1146-1149.

[26] 道客巴巴, “美国自行车巨头 Trek2008 年底推出无链自行车,” Doc88.com, 2016. <https://www.doc88.com/p-7186950817124.html> (accessed Dec. 01, 2025).

[27] 天空 ."CeramicSpeed DrivEn 全新传动体系 ." *中国自行车* .08(2018):77. doi:CNKI:SUN:GZXC.0.2018-08-015.

[28] 江国强."新式中轴传动机构." *中国自行车* .09(1999):31. doi:CNKI:SUN:GZXC.0.1999-09-024.

[29] MakelsanChain, “ROLLER CHAINS,” Makelsan Chain, Oct. 31, 2022. <https://www.makelsanchain.com/products/roller-chains/> (accessed May 04, 2026).

[30] “Bike Family,” ElliptiGO, May 27, 2022. <https://www.elliptigo.com/bike-family/#sec-elliptical-bikes> (accessed May 04, 2026).

[31] lzevon, “Row, Row, Row Your... Bike? - Bitness.com | Geek to the Core,” Bitness.com, Feb. 27, 2007. <https://www.bitness.com/row-row-row-your-bike/> (accessed May 04, 2026).

[32] Zhimg.com, 2026. https://pic4.zhimg.com/v2-07affc4759f97c1a2f75efea194f0a8f_1440w.jpg (accessed Apr. 22, 2026).

[33] 2012. "Developments in Bicycle Equipment and Its Role in Promoting Cycling as a Travel Mode", City Cycling, John Pucher, Ralph Buehler

[34] “U.S. Patent for Chainring Patent (Patent # 11,110,991 issued September 7, 2021) - Justia Patents Search,” Justia.com, Jul. 07, 2017. <https://patents.justia.com/patent/11110991> (accessed Apr. 29, 2026).